The SEK-1 p38 MAP kinase pathway modulates Gq signaling in *C. elegans*

Jill M. Hoyt, Samuel K. Wilson, Madhuri Kasa, Jeremy S. Rise,

Irini Topalidou, Michael Ailion

Department of Biochemistry, University of Washington, Seattle, WA, 98195

Running Title: SEK-1 modulates Gq signaling

key words: p38 MAPK pathway, Gq signaling, animal behavior, *C. elegans*

Corresponding author:
Michael Ailion
Department of Biochemistry
University of Washington
Box 357350
1705 NE Pacific St
Seattle, WA 98195
Phone: 206-685-0111
email: mailion@uw.edu

Abstract

Gq is a heterotrimeric G protein that is widely expressed in neurons and regulates neuronal activity. To identify pathways regulating neuronal Gq signaling we performed a forward genetic screen in *Caenorhabditis elegans* for suppressors of activated Gq. One of the suppressors is an allele of *sek-1*, which encodes a mitogen-activated protein kinase kinase (MAPKK) in the p38 MAPK pathway. Here we show that *sek-1* mutants have a slow locomotion rate and that *sek-1* acts in acetylcholine neurons to modulate both locomotion rate and Gq signaling. Furthermore, we find that *sek-1* acts in mature neurons to modulate locomotion. Using genetic and behavioral approaches we demonstrate that other components of the p38 MAPK pathway also play a positive role in modulating locomotion and Gq signaling. Finally, we find that mutants in the SEK-1 p38 MAPK pathway partially suppress an activated mutant of the sodium leak channel NCA-1/NALCN, a downstream target of Gq signaling. Our results suggest that the SEK-1 p38 pathway may modulate the output of Gq signaling through NCA-1.

Introduction

Gq is a widely expressed heterotrimeric G protein that regulates a variety of biological processes ranging from neurotransmission to cardiovascular pathophysiology (Sánchez-Fernández *et al.* 2014). In the canonical Gq pathway, Gq activates phospholipase Cβ (PLCβ), which cleaves phosphatidylinositol 4,5-bisphosphate (PIP_2) into the second messengers diacylglycerol (DAG) and inositol trisphosphate (IP_3) (Rhee 2001). In addition to PLCβ, other Gq effectors have been identified including kinases, such as protein kinase Cζ (PKCζ) and Bruton's tyrosine kinase (Btk) (Bence *et al.* 1997; García-Hoz *et al.* 2010; Vaqué *et al.* 2013), and guanine nucleotide exchange factors (GEFs) for the small GTPase Rho, such as Trio (Williams *et al.* 2007; Vaqué *et al.* 2013). These noncanonical effectors bridge the activation of Gq to other cellular signaling cascades.

In order to study noncanonical pathways downstream of Gq, we used the nematode *C. elegans* which has a single Gαq homolog (EGL-30) and conservation of the other components of the Gq signaling pathway (Koelle 2016). In neurons, EGL-30 signals through EGL-8 (PLCβ) (Lackner *et al.* 1999) and UNC-73 (ortholog of Trio RhoGEF) (Williams *et al.* 2007). UNC-73 activates RHO-1 (ortholog of RhoA), which has been shown to enhance neurotransmitter release through both diacylglycerol kinase (DGK-1)-dependent and DGK-1-independent pathways (McMullan *et al.* 2006).

To identify additional signaling pathways that modulate Gq signaling, we screened for suppressors of the activated Gq mutant *egl-30(tg26)* (Doi and Iwasaki 2002). *egl-30(tg26)* mutant animals exhibit hyperactive locomotion and a "loopy" posture in which worms have exaggerated, deep body bends and loop onto themselves (Bastiani *et al.*

2003; Topalidou *et al.* 2017). Here we identify one of the suppressors as a deletion allele in the gene *sek-1*. SEK-1 is a mitogen-activated protein kinase kinase (MAPKK), the *C. elegans* ortholog of mammalian MKK3/6 in the p38 MAPK pathway (Tanaka-Hino *et al.* 2002). The p38 MAPK pathway has been best characterized as a pathway activated by a variety of cellular stresses and inflammatory cytokines (Kyriakis and Avruch 2012). However, the p38 MAPK pathway has also been shown to be activated downstream of a G protein-coupled receptor in rat neurons (Huang *et al.* 2004). Btk, a member of the Tec family of tyrosine kinases, has been shown to act downstream of Gq to activate the p38 MAPK pathway (Bence *et al.* 1997), but *C. elegans* lacks Btk and other Tec family members (Plowman *et al.* 1999).

SEK-1 is activated by the MAPKKK NSY-1 (ortholog of ASK1) and activates the p38 MAPKs PMK-1 and PMK-2 (Andrusiak and Jin 2016). The p38 MAPK pathway consisting of NSY-1, SEK-1, and PMK-1 is required for innate immunity in *C. elegans* (Kim *et al.* 2002). NSY-1 and SEK-1 are also required for the specification of the asymmetric AWC olfactory neurons (Sagasti *et al.* 2001; Tanaka-Hino *et al.* 2002); the p38 orthologs PMK-1 and PMK-2 function redundantly in AWC specification (Pagano *et al.* 2015). For both innate immunity and AWC specification, the p38 MAPK pathway acts downstream of the adaptor protein TIR-1 (an ortholog of SARM) (Couillault *et al.* 2004; Chuang and Bargmann 2005). Here we show that the pathway consisting of TIR-1, NSY-1, SEK-1, PMK-1 and PMK-2 also acts to modulate locomotion downstream of Gq signaling.

Materials and Methods

C. elegans strains and maintenance

All strains were cultured using standard methods and maintained at 20°C (Brenner 1974). The *sek-1(yak42)* mutant was isolated from an ENU mutagenesis suppressor screen of the activated Gq mutant *egl-30(tg26)* (Ailion *et al.* 2014). *sek-1(yak42)* was outcrossed away from *egl-30(tg26)* before further analysis. Double mutant strains were constructed using standard methods (Fay 2006), often with linked fluorescent markers (Frokjaer-Jensen *et al.* 2014) to balance mutations with subtle visible phenotypes. Table S1 contains all the strains used in this study.

Mapping

yak42 was mapped using its slow locomotion phenotype and its *egl-30(tg26)* suppression phenotype. *yak42* was initially mapped to the X chromosome using strains EG1000 and EG1020, which carry visible marker mutations. These experiments showed that *yak42* was linked to *lon-2*, but at least several map units away. *yak42* was further mapped to about one map unit (m.u.) away from the red fluorescent insertion marker *oxTi668* which is located at +0.19 m.u. on the X chromosome.

Whole-genome sequencing

Strain XZ1233 *egl-30(tg26); yak42* was used for whole-genome sequencing to identify candidate *yak42* mutations. XZ1233 was constructed by crossing a 2X outcrossed *yak42* strain back to *egl-30(tg26)*. Thus, in XZ1233, *yak42* has been outcrossed 3X from its original isolate. DNA was isolated from XZ1233 and purified according to the Hobert Lab protocol (http://hobertlab.org/whole-genome-sequencing/).

Ion Torrent sequencing was performed at the University of Utah DNA Sequencing Core Facility. The resulting data contained 10,063,209 reads of a mean read length of 144 bases, resulting in about 14X average coverage of the *C. elegans* genome. The sequencing data were uploaded to the Galaxy web platform and we used the public server at usegalaxy.org to analyze the data (Afgan *et al.* 2016). We identified and annotated variants with the Unified Genotyper and SnpEff tools, respectively (DePristo *et al.* 2011; Cingolani *et al.* 2012). We filtered out variants found in other strains we sequenced, leaving us with 605 homozygous mutations. The X chromosome contained 94 mutations: 55 SNPs and 39 indels. Of these, four SNPs were non-synonymous mutations in protein-coding genes, but only two were within 5 m.u. of *oxTi668.* However, we were unable to identify *yak42* from the candidate polymorphisms located near *oxTi668*. Transgenic expression of the most promising candidate *pcyt-1* did not rescue *yak42*. Instead, to identify possible deletions, we scrolled through 2 MB of aligned reads on the UCSC Genome Browser starting at -4.38 m.u. and moving towards the middle of the chromosome (0 m.u.), looking for regions that lacked sequence coverage. We found a 3713 bp deletion that was subsequently confirmed to be the *yak42* causal mutation, affecting the gene *sek-1* located at -1.14 m.u.

Locomotion assays

Locomotion assay plates were made by seeding 10 cm nematode growth medium plates with 150 µl of an *E. coli* OP50 stock culture, spread with sterile glass beads to cover the entire plate. Bacterial lawns were grown at room temperature (22.5°C -24.5°C) for 24 hrs and then stored at 4°C until needed. All locomotion assays

were performed on first-day adults at room temperature (22.5°C -24.5°C). L4 stage larvae were picked the day before the assay and the experimenter was blind to the genotypes of the strains assayed. For experiments on strains carrying extrachromosomal arrays, the *sek-1(km4)* control worms were animals from the same plate that had lost the array.

Body bend assays were performed as described (Miller *et al.* 1999). A single animal was picked to the assay plate, the plate lid was returned, and the animal allowed to recover for 30 s. Body bends were then counted for one minute, counting each time the worm's tail reached the minimum or maximum amplitude of the sine wave. All strains in an experiment were assayed on the same assay plate. For experiments with *egl-8*, *unc-73*, and *rund-1* mutants, worms were allowed a minimal recovery period (until the worms started moving forward, 5 sec maximum) prior to counting body bends.

For the heat shock experiment, plates of first-day adults were parafilmed and heat-shocked in a 34°C water bath for 1 hr. Plates were then un-parafilmed and incubated at 20°C for five hours before performing body bend assays.

Radial locomotion assays were performed by picking animals to the middle of an assay plate. Assay plates were incubated at 20°C for 20 hr and the distances of the worms from the starting point were measured.

Quantitative analysis of the waveform of worm tracks was performed as described (Topalidou *et al.* 2017). Briefly, worm tracks were photographed and Image J was used to measure the period and amplitude. The value for each animal was the average of five period/amplitude ratios.

C. elegans pictures

Pictures of worms were taken at 60X on a Nikon SMZ18 microscope with the DS-L3 camera control system. The worms were age-matched as first-day adults and each experiment set was photographed on the same locomotion assay plate prepared as described above. The images were processed using ImageJ and were rotated, cropped, and converted to grayscale.

Molecular biology

Plasmids were constructed using the Gateway cloning system (Invitrogen). Plasmids and primers used are found in Table S2. The *sek-1* cDNA was amplified by RT-PCR from worm RNA and cloned into a Gateway entry vector. To ensure proper expression of *sek-1*, an operon GFP was included in expression constructs with the following template: (promoter)p::*sek-1*(cDNA)::*tbb-2utr::gpd-2 operon::GFP::H2B:cye-1utr* (Frøkjær-Jensen *et al.* 2012). This resulted in untagged SEK-1, but expression could be monitored by GFP expression.

Injections

C. elegans strains with extrachromosomal arrays were generated by standard methods (Mello *et al.* 1991). Injection mixes were made with a final total concentration of 100 ng/µL DNA. Constructs were injected at 5 ng/µL, injection markers at 5 ng/µL, and the carrier DNA Litmus 38i at 90 ng/µL. Multiple lines of animals carrying extrachromosomal arrays were isolated and had similar behaviors as observed by eye. The line with the highest transmittance of the array was assayed.

177

178 ***Statistical analysis***

179 At the beginning of the project, a power study was conducted on pilot body bend
180 assays using wild type and *sek-1(yak42)* worms. To achieve a power of 0.95, it was
181 calculated that 17 animals should be assayed per experiment. Data were analyzed to
182 check if normally distributed (using the D'Agostino-Pearson and Shapiro-Wilk normality
183 tests) and then subjected to the appropriate analysis using GraphPad Prism 5. For data
184 sets with three or more groups, if the data were normal they were analyzed with a one-
185 way ANOVA; if not, with a Kruskal-Wallis test. Post-hoc tests were used to compare
186 data sets within an experiment. Reported p-values are corrected. Table S3 contains the
187 statistical tests for each experiment. $p<0.05$ = *; $p<0.01$ = **; $p<0.001$ = ***.

188

189 ***Reagent and Data Availability***

190 Strains and plasmids are shown in Table S1 and Table S2 and are available from
191 the *Caenorhabditis* Genetics Center (CGC) or upon request. The authors state that all
192 data necessary for confirming the conclusions presented in the article are represented
193 fully within the article and Supplemental Material.

194

195 **Results**

196 ***sek-1* suppresses activated Gq**

197 To identify genes acting downstream of Gαq, we performed a forward genetic
198 screen for suppressors of the activated Gq mutant, *egl-30(tg26)* (Doi and Iwasaki 2002).
199 *egl-30(tg26)* worms are hyperactive and have a “loopy” posture characterized by an

exaggerated waveform (Figure 1B-1E). Thus, we screened for worms that are less hyperactive and less loopy. We isolated a recessive suppressor, *yak42*, and mapped it to the middle of the X chromosome (see Materials and Methods). Whole-genome sequencing revealed that *yak42* carries a large deletion of the *sek-1* gene from upstream of the start codon into exon 4 (Figure 1A). *yak42* also failed to complement *sek-1(km4)*, a previously published *sek-1* deletion allele, for the Gq suppression phenotype (Figure 1A) (Tanaka-Hino *et al.* 2002).

egl-30(tg26) double mutants with either *sek-1(yak42)* or *sek-1(km4)* are not loopy (Figure 1B-1D) and are not hyperactive (Figure 1E and S1A). *sek-1(yak42)* was outcrossed from *egl-30(tg26)* and assayed for locomotion defects. Both the *sek-1(yak42)* and *sek-1(km4)* mutants are coordinated but move more slowly than wild-type (Figure 1F). The *sek-1(ag1)* point mutation (Kim *et al.* 2002) also causes a similar slow locomotion phenotype (Figure S1B). To test whether the *egl-30(tg26)* suppression phenotype might be an indirect effect of the slow locomotion of a *sek-1* mutant, we built an *egl-30(tg26)* double mutant with a mutation in *unc-82*, a gene required for normal muscle structure. *unc-82* mutants are coordinated but move slowly, similar to a *sek-1* mutant (Hoppe *et al.* 2010). However, although an *egl-30(tg26) unc-82(e1220)* double mutant moves more slowly than *egl-30(tg26)* (Figure S1C), it is still loopy (Figure 1B-1D). Thus, *sek-1* appears to be a specific suppressor of activated *egl-30*.

The *egl-30(tg26)* allele causes an R243Q missense mutation in the Gα switch III region that has been shown to reduce both the intrinsic GTPase activity of the G protein and render it insensitive to GTPase-activation by a regulator of G protein signaling (RGS) protein, thus leading to increased G protein activation (Natochin and Artemyev

2003). To test whether the suppression of *egl-30(tg26)* by *sek-1* is specific for this *egl-30* allele, we built a double mutant between *sek-1(km4)* and the weaker activating mutation *egl30(js126)*. *egl-30(js126)* causes a V180M missense mutation in the Gα switch I region immediately adjacent to one of the key residues required for GTPase catalysis (Hawasli *et al.* 2004). Thus, the *tg26* and *js126* alleles activate EGL-30 through different mechanisms. The *sek-1(km4)* mutant also suppresses the hyperactivity and loopy waveform of *egl-30(js126)* (Figure 1G, 1H), demonstrating that *sek-1* suppression of activated *egl-30* is not allele-specific.

EGL-30/Gαq is negatively regulated by GOA-1, the worm Gαo/i ortholog, and the RGS protein EAT-16 (Hajdu-Cronin *et al.* 1999). We tested whether *sek-1* also suppresses the *goa-1* and *eat-16* loss-of-function mutants that cause a hyperactive and loopy phenotype similar to activated *egl-30* mutants. *sek-1(km4)* suppresses the hyperactivity and loopy waveform of *goa-1(sa734)* (Figure S1D, S1E). However, though *sek-1(km4)* suppresses the hyperactivity of *eat-16(tm775)*, it did not significantly suppress the loopy waveform (Figure S1F, S1G). One possible downstream effector of GOA-1 is the DAG kinase DGK-1 that inhibits DAG-dependent functions such as synaptic vesicle release (Nurrish *et al.* 1999; Miller *et al.* 1999). *dgk-1(sy428)* animals are hyperactive, but the *sek-1 dgk-1* double mutant is uncoordinated and looks like neither *sek-1* nor *dgk-1* mutants, confounding the interpretation of how *sek-1* genetically interacts with *dgk-1*.

sek-1 acts in mature acetylcholine neurons

245 *egl-30* is widely expressed and acts in neurons to modulate locomotion (Lackner
246 *et al.* 1999), so it is possible that *sek-1* also acts in neurons to modulate Gq signaling.
247 *sek-1* is expressed in neurons, intestine, and several other tissues (Tanaka-Hino *et al.*
248 2002) and has been shown to function in GABA neurons to promote synaptic
249 transmission (Vashlishan *et al.* 2008).
250 To identify the cell type responsible for the *sek-1* locomotion phenotypes, we
251 expressed the wild-type *sek-1* cDNA under different cell-specific promoters and tested
252 for transgenic rescue of a *sek-1* null mutant. Expression of *sek-1* in all neurons (using
253 the *unc-119* promoter) or in acetylcholine neurons (*unc-17* promoter) was sufficient to
254 rescue the *sek-1* mutant slow locomotion phenotype, but expression in GABA neurons
255 (*unc-47* promoter) was not sufficient to rescue (Figure 2A, B). These results indicate
256 that *sek-1* acts in acetylcholine neurons to modulate locomotion rate.
257 We next tested whether *sek-1* acts in neurons to suppress *egl-30(tg26)*.
258 Expression of *sek-1* under pan-neuronal and acetylcholine neuron promoters reversed
259 the *sek-1* suppression of *egl-30(tg26)*. Specifically, *egl-30(tg26) sek-1* double mutants
260 expressing wild-type *sek-1* in all neurons or acetylcholine neurons resembled the *egl-*
261 *30(tg26)* single mutant (Figure 2C-E). However, expression of *sek-1* in GABA neurons
262 did not reverse the suppression phenotype (Figure 2C-E). Together, these data show
263 that *sek-1* acts in acetylcholine and not GABA neurons to modulate both wild-type
264 locomotion rate and to modulate Gq signaling.
265 To narrow down the site of *sek-1* action, we expressed *sek-1* in head (*unc-17H*
266 promoter) and motorneuron (*unc-17β* promoter) acetylcholine neuron subclasses
267 (Topalidou *et al.* 2017). Expression of *sek-1* in acetylcholine motorneurons rescued the

sek-1 slow locomotion phenotype (Figure S2A), suggesting that the slow locomotion of *sek-1* mutants is due to a loss of *sek-1* in acetylcholine motorneurons. However, expression of *sek-1* in either the head acetylcholine neurons or motorneurons partially reversed the *sek-1* suppression of *egl-30(tg26)* hyperactivity (Figure S2B), suggesting that the hyperactivity of activated Gq mutants may result from excessive Gq signaling in both head acetylcholine neurons and acetylcholine motorneurons; *sek-1* may act in Gq signaling in both neuronal cell types. By contrast, expression of *sek-1* in head acetylcholine neurons but not motorneurons reversed the *sek-1* suppression of the *egl-30(tg26)* loopy waveform (Figure S2C), suggesting that the loopy posture of activated Gq mutants may result from excessive Gq signaling in head acetylcholine neurons, and *sek-1* may act in those neurons to control body posture.

Because *sek-1* acts in the development of the AWC asymmetric neurons, we asked whether *sek-1* also has a developmental role in modulating locomotion by testing whether adult-specific *sek-1* expression (driven by a heat-shock promoter) is sufficient to rescue the *sek-1* mutant. We found that *sek-1* expression in adults rescues the *sek-1* slow locomotion phenotype (Figure 2F). This result indicates that *sek-1* is not required for development of the locomotion circuit and instead acts in mature neurons to modulate locomotion.

The p38 MAPK pathway is a positive regulator of Gq signaling

SEK-1 is the MAPKK in the p38 MAPK pathway consisting of the adaptor protein TIR-1, NSY-1 (MAPKKK), SEK-1 (MAPKK), and PMK-1 or PMK-2 (MAPKs) (Tanaka-Hino *et al.* 2002; Andrusiak and Jin 2016). We tested whether the entire p38 MAPK

signaling module also modulates locomotion rate and suppression of activated Gq. Both *tir-1(tm3036)* and *nsy-1(ok593)* mutant animals have slow locomotion on their own and also suppress the hyperactivity and loopy waveform of *egl-30(tg26)* (Figure 3A-D, G and H). We also tested single mutants in each of the three worm p38 MAPK genes (*pmk-1, pmk-2* and *pmk-3)* and a *pmk-2 pmk-1* double mutant. Although we found that the *pmk-2* and *pmk-3* single mutants were slightly slow on their own, only the *pmk-2 pmk-1* double mutant phenocopied *sek-1* and suppressed both the hyperactivity and loopy waveform of *egl-30(tg26)* (Figure 3E-H). Thus, *pmk-2* and *pmk-1* act redundantly downstream of *sek-1* to suppress *egl-30(tg26).* These data suggest that the p38 MAPK pathway modulates locomotion rate in *C. elegans* and acts genetically downstream of *egl-30*.

The JNK MAPK pathway, related to the p38 MAPK family, also modulates locomotion in *C. elegans*. Specifically, the JNK pathway members *jkk-1* (JNK MAPKK) and *jnk-1* (JNK MAPK) have been shown to act in GABA neurons to modulate locomotion (Kawasaki 1999). We found that the *jkk-1* and *jnk-1* single mutants had slow locomotion and that the double mutants with p38 MAPK pathway members exhibited an additive slow locomotion phenotype (Figure S3A). Moreover, neither *jkk-1* nor *jnk-1* suppressed the loopy phenotype of *egl-30(tg26)* (Figure S3B). Thus, the JNK and p38 MAPK pathways modulate locomotion independently and the JNK pathway is not involved in Gq signaling.

We also tested the involvement of possible p38 MAPK pathway effectors. One of the targets of PMK-1 is the transcription factor ATF-7 (Shivers *et al.* 2010). Both the *atf-7(qd22 qd130)* loss-of-function mutant and the *atf-7(qd22)* gain-of-function mutant

314 moved slowly compared to wild-type animals (Figure S3C). However, *atf-7(qd22 qd130)*
315 did not suppress the loopiness of *egl-30(tg26)* (Figure S3B), suggesting that *atf-7* is not
316 a target of this pathway, or else it acts redundantly with other downstream p38 MAPK
317 targets. We also tested *gap-2*, the closest *C. elegans* homolog of ASK1-interacting
318 Protein (AIP1) which activates ASK1 (the ortholog of *C. elegans* NSY-1) in mammalian
319 systems (Zhang *et al.* 2003). A *C. elegans gap-2* mutant has no locomotion defect
320 (Figure S3D). Finally, we tested VHP-1, a phosphatase for p38 and JNK MAPKs that
321 inhibits p38 MAPK signaling (Kim *et al.* 2004). However, the *vhp-1(sa366)* mutant also
322 has no locomotion defect (Figure S3D).

323 *egl-30(tg26)* animals are loopy and hyperactive so we tested whether increased
324 activation of the TIR-1/p38 MAPK signaling module causes similar phenotypes. The *tir-*
325 *1(ky648tg26)* allele leads to a gain-of-function phenotype in the AWC neuron
326 specification (Chang *et al.* 2011), but does not cause loopy or hyperactive locomotion
327 (Figure S3E, F).

328

329 **Genetic interactions of *sek-1* with pathways acting downstream of Gq**

330 Our forward genetic screen for suppressors of *egl-30(tg26)* identified mutants
331 that fall into three different categories: mutants in the canonical Gq pathway such as the
332 PLC *egl-8* ((Lackner *et al.* 1999), mutants in the RhoGEF Trio pathway such as *unc-73*
333 (Williams et al., 2007), and mutants that affect dense-core vesicle biogenesis and
334 release (Ailion *et al.* 2014; Topalidou *et al.* 2016).

335 To test if *sek-1* acts in any of these pathways we built double mutants between
336 *sek-1* and members of each pathway. Loss-of-function alleles of *egl-8(sa47)*, *unc-*

337 *73(ox317),* and *rund-1(tm3622)* have slow locomotion (Figure 4A-C). We found that
338 *sek-1* enhances the slow locomotion phenotype of *egl-8* and *rund-1* single mutants,
339 suggesting that *sek-1* does not act in the same pathway as *egl-8* or *rund-1* (Figure 4A,
340 B). By contrast, *sek-1* does not enhance the slow locomotion phenotype of *unc-73*
341 mutants (Figure 4C), suggesting that *sek-1* may act in the same genetic pathway as the
342 Trio RhoGEF *unc-73.*

343 We next tested whether *sek-1* interacts with *rho-1*, encoding the small G protein
344 Rho that is activated by Trio. Because *rho-1* is required for viability (Jantsch-Plunger *et*
345 *al.* 2000), we used an integrated transgene overexpressing an activated *rho-1* mutant
346 allele specifically in acetylcholine neurons. Animals carrying this activated RHO-1
347 transgene, referred to here as *rho-1(gf)*, have a loopy posture reminiscent of *egl-*
348 *30(tg26)* (McMullan *et al.* 2006), and a decreased locomotion rate (Figure 4D-F). *rho-*
349 *1(gf) sek-1(km4)* double mutants had a loopy body posture like *rho-1(gf)* and an even
350 slower locomotion rate (Figure 4D-F), suggesting that *sek-1* and *rho-1(gf)* mutants have
351 additive locomotion phenotypes. However, both *sek-1(km4)* and *sek-1(yak42)* weakly
352 suppress the slow growth rate of the *rho-1(gf)* mutant (data not shown). Because *sek-1*
353 does not enhance *unc-73* mutants and suppresses some aspects of the *rho-1(gf)*
354 mutant, *sek-1* may modulate output of the Rho pathway, though it probably is not a
355 direct transducer of Rho signaling.
356

357 **_sek-1_ and _nsy-1_ partially suppress activated NCA**

358 To clarify the relationship of the SEK-1 p38 MAPK pathway to the Rho pathway
359 acting downstream of Gq, we examined interactions with *nca-1*, a downstream target of

the Gq-Rho pathway (Topalidou *et al.* 2017). NCA-1 and its orthologs are sodium leak channels associated with rhythmic behaviors in several organisms (Nash *et al.* 2002; Lu *et al.* 2007; Shi *et al.* 2016). In *C. elegans*, NCA-1 potentiates persistent motor circuit activity and sustains locomotion (Gao *et al.* 2015).

We tested whether *sek-1* and *nsy-1* mutants suppress the activated NCA-1 mutant *ox352*, referred to as *nca-1(gf)*. The *nca-1(gf)* animals are coiled and uncoordinated; thus, it is difficult to measure their locomotion rate by the body bend assay because they do not reliably propagate sinusoidal waves down the entire length of their body. Instead, we used a radial locomotion assay in which we measured the distance animals moved from the center of a plate. *nca-1(gf)* double mutants with either *sek-1(km4)* or *nsy-1(ok593)* uncoil a bit but still exhibit uncoordinated locomotion (Figure 5A). In fact, though these double mutants show more movement in the anterior half of their bodies than *nca-1(gf)*, they propagate body waves to their posterior half even more poorly than the *nca-1(gf)* mutant. However, both *sek-1* and *nsy-1* partially suppress the loopy waveform of the *nca-1(gf)* mutant (Figure 5A, B) and in radial locomotion assays, *sek-1* and *nsy-1* weakly suppressed the *nca-1(gf)* locomotion defect (Figure 5C). Additionally, both *sek-1* and *nsy-1* partially suppress the small body size of *nca-1(gf)* (Figure S4A). Together these data suggest that mutations in the SEK-1 p38 MAPK pathway suppress some aspects of the *nca-1(gf)* mutant.

Given that *sek-1* acts in acetylcholine neurons to modulate wild-type and *egl-30(tg26)* locomotion, we tested whether *sek-1* also acts in these neurons to suppress *nca-1(gf)*. Expression of *sek-1* in all neurons or in acetylcholine neurons of *nca-1(gf) sek-1(km4)* animals restored the *nca-1(gf)* loopy phenotype (Figure 5D, E). By contrast,

383 expression of *sek-1* in GABA neurons did not affect the loopy posture of the *nca-1(gf)*
384 *sek-1* double mutant (Figure 5D, E). These data suggest that *sek-1* acts in acetylcholine
385 neurons to modulate the body posture of *nca-1(gf)* as well. However, in radial
386 locomotion assays, expression of *sek-1* in none of these neuron classes significantly
387 altered the movement of the *nca-1(gf) sek-1* double mutant (Figure S4B), though the
388 weak suppression of *nca-1(gf)* by *sek-1* in this assay makes it difficult to interpret these
389 negative results. To further narrow down the site of action of *sek-1* for its NCA
390 suppression phenotypes, we expressed it in subclasses of acetylcholine neurons.
391 Surprisingly, expression of *sek-1* in acetylcholine motorneurons but not head
392 acetylcholine neurons was sufficient to restore the loopy posture of the *nca-1(gf)* mutant
393 (Figure 5E), the opposite of what we found for *sek-1* modulation of the loopy posture of
394 the activated Gq mutant, suggesting that the loopy posture of *nca-1(gf)* mutants may
395 result from excessive NCA-1 activity in acetylcholine motorneurons. Additionally,
396 expression of *sek-1* in either the head acetylcholine neurons or the motorneurons
397 restored the *nca-1(gf)* small body size phenotype (Figure S4C). We make the tentative
398 conclusion that *sek-1* acts in acetylcholine neurons to modulate *nca-1(gf)* body posture
399 and size, but we were not able to conclusively narrow down its site of action further,
400 possibly due to the uncoordinated phenotype of *nca-1(gf)* and the weaker suppression
401 of *nca-1(gf)* by *sek-1* .
402
403 **Discussion**
404 The p38 MAPK pathway has been best characterized as a pathway activated by
405 a variety of cellular stresses and inflammatory cytokines (Kyriakis and Avruch 2012), but

406 it has also been implicated in neuronal function, including some forms of mammalian
407 synaptic plasticity (Bolshakov *et al.* 2000; Rush *et al.* 2002; Huang *et al.* 2004). In this
408 study we identified a new neuronal role for the mitogen-activated protein kinase kinase
409 SEK-1 and the p38 MAPK pathway as a positive modulator of locomotion rate and Gq
410 signaling. The physiological importance of this pathway is clear under conditions of
411 elevated Gq signaling but is less obvious during normal wild-type locomotion, consistent
412 with the observation that *sek-1* mutations have a relatively weak effect on synaptic
413 transmission in a wild-type background (Vashlishan *et al.* 2008). Thus, the SEK-1 p38
414 MAPK pathway may be more important for modulation of Gq signaling and synaptic
415 strength than for synaptic transmission per se.
416 In addition to SEK-1, we identified other p38 pathway components that modulate
417 Gq signaling. Specifically, we found that *tir-1, nsy-1* and *pmk-1 pmk-2* mutants exhibit
418 locomotion defects identical to *sek-1* and suppress activated Gq, suggesting that they
419 act in a single p38 pathway to modulate signaling downstream of Gq. These results
420 indicate a redundant function for PMK-1 and PMK-2 in modulating locomotion rate and
421 Gq signaling. PMK-1 and PMK-2 also act redundantly for some other neuronal roles of
422 the p38 pathway, such as the development of the asymmetric AWC neurons and to
423 regulate induction of serotonin biosynthesis in the ADF neurons in response to
424 pathogenic bacteria (Shivers *et al.* 2009; Pagano *et al.* 2015). By contrast, PMK-1 acts
425 alone in the intestine to regulate innate immunity and in interneurons to regulate
426 trafficking of the GLR-1 glutamate receptor (Pagano *et al.* 2015; Park and Rongo 2016).
427 What are the downstream effectors of the SEK-1 p38 MAPK pathway that
428 modulates locomotion? There are several known downstream effectors of p38 MAPK

signaling in *C. elegans*, including the transcription factor ATF-7 (Shivers *et al.* 2010). Our data indicate that ATF-7 is not required for the p38 MAPK-dependent modulation of Gq signaling. The p38 MAPK pathway may activate molecules other than transcription factors or may activate multiple downstream effectors.

How does the SEK-1 p38 pathway modulate the output of Gq signaling? One of the pathways that transduces signals from Gq includes the RhoGEF Trio/UNC-73, the small GTPase Rho, and the cation channel NALCN/NCA-1 (Williams *et al.* 2007; Topalidou *et al.* 2017). Compared to other pathways downstream of Gq, mutants in the Rho-Nca pathway are particularly strong suppressors of the loopy waveform phenotype of the activated Gq mutant (Topalidou *et al.* 2017). Similary, we found that mutations in the SEK-1 p38 MAPK pathway strongly suppress the loopy waveform of the activated Gq mutant, suggesting that the SEK-1 pathway might modulate Gq signal output through the Rho-Nca branch. Consistent with this, we found that mutations in the SEK-1 p38 MAPK pathway partially suppress an activated NCA-1 mutant. Given the precedence for direct phosphorylation of sodium channels by p38 to regulate channel properties (Wittmack *et al.* 2005; Hudmon *et al.* 2008), it is possible that PMK-1 and PMK-2 phosphorylate NCA-1 to regulate its expression, localization, or activity.

Consistent with the observation that Gq acts in acetylcholine neurons to stimulate synaptic transmission (Lackner *et al.* 1999), we found that *sek-1* acts in acetylcholine neurons to modulate the locomotion rate in both wild-type and activated Gq mutants. *sek-1* also acts in acetylcholine neurons to modulate the loopy waveform of both activated Gq and activated *nca-1* mutants, and the size of activated *nca-1* mutants. However, our data attempting to narrow down the site of action of *sek-1* suggest that it

452 may act in both head acetylcholine neurons and acetylcholine motorneurons, and that
453 the waveform is probably controlled by at least partially distinct neurons from those that
454 control locomotion rate. Further work will be required to identify the specific neurons
455 where Gq, NCA-1 and the SEK-1 pathway act to modulate locomotion rate and
456 waveform, and determine whether they all act together in the same cell.
457
458 **Acknowledgements**
459 We thank Dennis Kim and Chiou-Fen Chuang for strains, Pin-An Chen and Erik
460 Jorgensen for the *nca-1(gf)* mutant *ox352*, Chris Johnson for the fine mapping of *yak42*,
461 Jordan Hoyt for help with Galaxy to analyze WGS data, and Dana Miller for providing
462 access to her microscope camera. Some strains were provided by the CGC, which is
463 funded by NIH Office of Research Infrastructure Programs (P40 OD010440). J.M.H was
464 supported in part by Public Health Service, National Research Service Award
465 T32GM007270, from the National Institute of General Medical Sciences. M.A. is an
466 Ellison Medical Foundation New Scholar. This work was supported by NIH grant R00
467 MH082109 to M.A.
468
469 **Figure Legends**
470 **Figure 1. *sek-1* acts downstream of Gαq to modulate locomotion behavior**
471 (A) Gene structure of *sek-1*. White boxes depict the 5' and 3' untranslated regions,
472 black boxes depict exons, and lines show introns. The positions of the *yak42* and *km4*
473 deletions are shown. *yak42* is a 3713 bp deletion that extends to 1926 bp upstream of

the start codon. Drawn with Exon-Intron Graphic Maker (http://www.wormweb.org/exonintron). Scale bar is 100 bp.

(B-D) *sek-1(yak42)* and *sek-1(km4)* suppress the loopy waveform of the activated Gq mutant *egl-30(tg26). unc-82(e1220)* does not suppress *egl-30(tg26).* (B) Photos of first-day adult worms. WT: wild type. (C) Quantification of the waveform phenotype. ***, p<0.001; ns, p>0.05 compared to *egl-30(tg26)*. Error bars = SEM, n=5. (D) Photos of worm tracks.

(E) The activated Gq mutant *egl-30(tg26)* is hyperactive and is suppressed by *sek-1(yak42)* and *sek-1(km4)*. ***, p<0.001, error bars = SEM, n=20.

(F) *sek-1* mutant worms have slow locomotion. ***, p<0.001 compared to wild-type. Error bars = SEM, n=20.

(G) *sek-1(km4)* suppresses the hyperactive locomotion of the activated Gq mutant *egl-30(js126)*. ***, p<0.001, error bars = SEM, n=20.

(H) *sek-1(km4)* suppresses the loopy waveform of the activated Gq mutant *egl-30(js126)*. ***, p<0.001, error bars = SEM, n=5.

Figure 2. *sek-1* acts in mature acetylcholine neurons to modulate locomotion

(A) *sek-1* acts in neurons to modulate locomotion rate. The *sek-1* wild-type cDNA driven by the *unc-119* pan-neuronal promoter *[unc-119p::sek-1(+)]* rescues the slow locomotion phenotype of *sek-1(km4)* worms. ***, p< 0.001, error bars = SEM, n=20.

(B) *sek-1* acts in acetylcholine neurons to modulate locomotion rate. *sek-1* WT cDNA driven by the *unc-17* acetylcholine neuron promoter *[unc-17p::sek-1(+)]* rescues the slow locomotion phenotype of *sek-1(km4)* worms but *sek-1* expression in GABA

neurons using the *unc-47* promoter *[unc-47p::sek-1(+)]* does not. ***, p< 0.001, error bars = SEM, n=20.

(C-D) *sek-1* acts in acetylcholine neurons to modulate the loopy waveform of *egl-30(tg26). egl-30(tg26) sek-1(km4)* worms expressing *unc-119p::sek-1(+)* or *unc-17p::sek-1(+)* are loopy like *egl-30(tg26)*, but *egl-30(tg26) sek-1(km4)* worms expressing *unc-47p::sek-1(+)* are similar to *egl-30(tg26) sek-1.* (C) Photos of worms. (D) Quantification of waveform phenotype. ***, p<0.001; ns, p>0.05. Error bars = SEM, n=5.

(E) *sek-1* acts in acetylcholine neurons to modulate the locomotion rate of *egl-30(tg26). egl-30(tg26) sek-1(km4)* worms expressing *unc-119p::sek-1(+)* or *unc-17p::sek-1(+)* have an increased locomotion rate compared to *egl-30(tg26) sek-1*, but *egl-30(tg26) sek-1(km4)* worms expressing *unc-47p::sek-1(+)* are similar to *egl-30(tg26) sek-1.* ***, p< 0.001, **, p<0.01; ns, p>0.05. Error bars = SEM, n=17-20.

(F) *sek-1* acts in mature neurons to modulate locomotion rate. Heat-shock induced expression of *sek-1* in adults (*hsp-16.2p::sek-1(+)*) rescues the slow locomotion phenotype of *sek-1(km4)*. ***, p< 0.001, error bars = SEM, n=20.

Figure 3. The p38 MAPK pathway modulates locomotion downstream of *egl-30*

(A) *tir-1(tm3036)* mutant animals have slow locomotion. ***, p<0.001, error bars = SEM, n=20.

(B) *tir-1(tm3036)* suppresses *egl-30(tg26)*. *egl-30(tg26) tir-1* animals move more slowly than the hyperactive *egl-30(tg26)* animals. ***, p< 0.001, error bars = SEM, n=20.

(C) *nsy-1(ok593)* mutant animals have slow locomotion. ***, p<0.001, error bars = SEM, n=20.

(D) *nsy-1(ok593)* suppresses *egl-30(tg26)*. *egl-30(tg26) nsy-1* animals move more slowly than the hyperactive *egl-30(tg26)* animals. ***, p< 0.001, error bars = SEM, n=20.

(E) *pmk-2, pmk-2 pmk-1,* and *pmk-3* mutant animals have slow locomotion. ***, p< 0.001; *, p<0.05, compared to WT. Error bars = SEM, n=20.

(F) A *pmk-2 pmk-1* double mutant suppresses the hyperactivity of *egl-30(tg26)*. ***, p< 0.001 compared to *egl-30(tg26)*. Error bars = SEM, n=20.

(G, H) *tir-1(tm3036)*, *nsy-1(ok593)*, and the *pmk-2 pmk-1* double mutant suppress the loopy waveform of *egl-30(tg26)*. *egl-30(tg26)* animals with mutations in either *pmk-1, pmk-2,* or *pmk-3* are still loopy. (G) Worm photos. (H) Quantification. ***, p<0.001 compared to *egl-30(tg26)*. Error bars = SEM, n=5.

Figure 4. *sek-1* acts in the same genetic pathway as *unc-73*

(A) *sek-1* does not act in the same genetic pathway as *egl-8.* The *sek-1(yak42)* mutation enhances the slow locomotion of the *egl-8(sa47)* mutant. ***, p< 0.001, error bars = SEM, n=20.

(B) *sek-1* does not act in the same genetic pathway as *rund-1*. The *sek-1(yak42)* mutation enhances the slow locomotion of the *rund-1(tm3622)* mutant. ***, p< 0.001, error bars = SEM, n=20.

(C) *sek-1* may act in the same genetic pathway as *unc-73*. The *sek-1(yak42)* mutation does not enhance the slow locomotion phenotype of the *unc-73(ox317)* mutant. ns, p>0.05, error bars = SEM, n=20.

(D-E) *sek-1(km4)* does not suppress the loopy waveform of *nzIs29 rho-1(gf)* animals. (D) Worm photos. (E) Quantification. ns, p>0.05, error bars = SEM, n=5.

(F) *sek-1(km4)* does not suppress the slow locomotion of *rho-1(gf)* animals. ***, p< 0.001, error bars = SEM, n=20.

Figure 5. *sek-1* and *nsy-1* weakly suppress *nca-1(gf)*

(A) *nca-1(gf)* mutants are small, loopy, and uncoordinated. The phenotypes of *nca-1(ox352)* animals are partially suppressed by *sek-1(km4)* and *nsy-1(ok593)*. Photos of first-day adults.

(B) *sek-1(km4)* and *nsy-1(ok593)* suppress the loopy waveform of *nca-1(gf)*. ***, p<0.001; **, p<0.01. Error bars = SEM, n=5.

(C) *sek-1* and *nsy-1* suppress *nca-1(gf)* locomotion. *nca-1(gf)* animals travel a small distance from the center of the plate in the radial locomotion assay. *nca-1(gf) nsy-1(ok593)* and *nca-1(gf) sek-1(km4)* worms move further than *nca-1(gf)* worms. **, p<0.01; *, p<0.05. Error bars = SEM, n=30.

(D) *sek-1* acts in acetylcholine neurons to modulate the size and loopy waveform of *nca-1(gf)*. *nca-1(ox352) sek-1(km4)* animals expressing *sek-1* in all neurons (*unc-119p::sek-1(+)*) or in acetylcholine neurons (*unc-17p::sek-1(+)*) are loopy and small like *nca-1(gf)*, but *nca-1(ox352) sek-1(km4)* animals expressing *sek-1* in GABA neurons (*unc-47p::sek-1(+)*) resemble *nca-1(gf) sek-1*. White arrowheads depict food piles created by *nca-1(gf) sek-1(km4)* animals due to their uncoordinated locomotion. Such food piles are not made by *nca-1(gf)* animals.

(E) *sek-1* acts in acetylcholine motorneurons to modulate the loopy waveform of *nca-1(gf)*. *nca-1(ox352) sek-1(km4)* worms expressing *sek-1* in all neurons (*unc-119p::sek-1(+)*), acetylcholine neurons (*unc-17p::sek-1(+)*), or acetylcholine motorneurons (*unc-*

566 *17βp::sek-1(+)*) are loopy like *nca-1(gf)*, but *nca-1(ox352) sek-1(km4)* worms expressing
567 *sek-1* in GABA neurons (*unc-47p::sek-1(+)*) or head acetylcholine neurons (*unc-*
568 *17Hp::sek-1(+)*) are similar to *nca-1(gf) sek-1*. ***, p< 0.001, **, p<0.01; ns, p>0.05.
569 Error bars = SEM, n=5.
570

571 **References**

572 Afgan, E., D. Baker, M. van den Beek, D. Blankenberg, D. Bouvier *et al.*, 2016 The
573 Galaxy platform for accessible, reproducible and collaborative biomedical
574 analyses: 2016 update. Nucleic Acids Res. 44: W3–W10.

575 Ailion, M., M. Hannemann, S. Dalton, A. Pappas, S. Watanabe *et al.*, 2014 Two Rab2
576 interactors regulate dense-core vesicle maturation. Neuron 82: 167–180.

577 Andrusiak, M. G., and Y. Jin, 2016 Context Specificity of Stress-activated Mitogen-
578 activated Protein (MAP) Kinase Signaling: The Story as Told by Caenorhabditis
579 elegans. J. Biol. Chem. 291: 7796–7804.

580 Bastiani, C. A., S. Gharib, M. I. Simon, and P. W. Sternberg, 2003 Caenorhabditis
581 elegans Gαq Regulates Egg-Laying Behavior via a PLCβ-Independent and
582 Serotonin-Dependent Signaling Pathway and Likely Functions Both in the
583 Nervous System and in Muscle. Genetics 165: 1805–1822.

584 Bence, K., W. Ma, T. Kozasa, and X.-Y. Huang, 1997 Direct stimulation of Bruton's
585 tyrosine kinase by Gq-protein α-subunit. Nature 389: 296–299.

586 Bolshakov, V. Y., L. Carboni, M. H. Cobb, S. A. Siegelbaum, and F. Belardetti, 2000
587 Dual MAP kinase pathways mediate opposing forms of long-term plasticity at
588 CA3-CA1 synapses. Nat. Neurosci. 3: 1107–1112.

589 Brenner, S., 1974 The genetics of Caenorhabditis elegans. Genetics 77: 71–94.

590 Chang, C., Y.-W. Hsieh, B. J. Lesch, C. I. Bargmann, and C.-F. Chuang, 2011
591 Microtubule-based localization of a synaptic calcium-signaling complex is
592 required for left-right neuronal asymmetry in C. elegans. Development 138:
593 3509–3518.

594 Chuang, C.-F., and C. I. Bargmann, 2005 A Toll-interleukin 1 repeat protein at the
595 synapse specifies asymmetric odorant receptor expression via ASK1 MAPKKK
596 signaling. Genes Dev. 19: 270–281.

597 Cingolani, P., A. Platts, L. L. Wang, M. Coon, T. Nguyen *et al.*, 2012 A program for
598 annotating and predicting the effects of single nucleotide polymorphisms, SnpEff:
599 SNPs in the genome of Drosophila melanogaster strain w1118; iso-2; iso-3. Fly
600 6: 80–92.

601 Couillault, C., N. Pujol, J. Reboul, L. Sabatier, J.-F. Guichou *et al.*, 2004 TLR-
602 independent control of innate immunity in Caenorhabditis elegans by the TIR
603 domain adaptor protein TIR-1, an ortholog of human SARM. Nat. Immunol. 5:
604 488–494.

605 DePristo, M. A., E. Banks, R. Poplin, K. V. Garimella, J. R. Maguire *et al.*, 2011 A
606 framework for variation discovery and genotyping using next-generation DNA
607 sequencing data. Nat. Genet. 43: 491–498.

608 Doi, M., and K. Iwasaki, 2002 Regulation of retrograde signaling at neuromuscular
609 junctions by the novel C2 domain protein AEX-1. Neuron 33: 249–259.

610 Fay, D., 2006 Genetic mapping and manipulation: Chapter 7-Making compound
611 mutants. *WormBook*, ed. The *C. elegans* Research Community, WormBook,
612 doi/10.1895/wormbook.1.96.2, http://www.wormbook.org

613 Frøkjær-Jensen, C., M. W. Davis, M. Ailion, and E. M. Jorgensen, 2012 Improved
614 Mos1-mediated transgenesis in C. elegans. Nat. Methods 9: 117–118.

615 Frokjaer-Jensen, C., M. W. Davis, M. Sarov, J. Taylor, S. Flibotte *et al.*, 2014 Random
616 and targeted transgene insertion in C. elegans using a modified Mosl transposon.
617 Nat. Methods 11: 529–534.

618 Gao, S., L. Xie, T. Kawano, M. D. Po, J. K. Pirri *et al.*, 2015 The NCA sodium leak
619 channel is required for persistent motor circuit activity that sustains locomotion.
620 Nat. Commun. 6: 6323.

621 García-Hoz, C., G. Sánchez-Fernández, M. T. Díaz-Meco, J. Moscat, F. Mayor *et al.*,
622 2010 Gαq Acts as an Adaptor Protein in Protein Kinase Cζ (PKCζ)-mediated
623 ERK5 Activation by G Protein-coupled Receptors (GPCR). J. Biol. Chem. 285:
624 13480–13489.

625 Hajdu-Cronin, Y. M., W. J. Chen, G. Patikoglou, M. R. Koelle, and P. W. Sternberg,
626 1999 Antagonism between Goα and Gqα in Caenorhabditis elegans: the RGS
627 protein EAT-16 is necessary for Goα signaling and regulates Gqα activity. Genes
628 Dev. 13: 1780–1793.

629 Hawasli, A. H., O. Saifee, C. Liu, M. L. Nonet, and C. M. Crowder, 2004 Resistance to
630 volatile anesthetics by mutations enhancing excitatory neurotransmitter release
631 in Caenorhabditis elegans. Genetics 168: 831–843.

632 Hoppe, P. E., J. Chau, K. A. Flanagan, A. R. Reedy, and L. A. Schriefer, 2010
633 Caenorhabditis elegans unc-82 Encodes a Serine/Threonine Kinase Important
634 for Myosin Filament Organization in Muscle During Growth. Genetics 184: 79–90.

635 Huang, C.-C., J.-L. You, M.-Y. Wu, and K.-S. Hsu, 2004 Rap1-induced p38 mitogen-
636 activated protein kinase activation facilitates AMPA receptor trafficking via the
637 GDI.Rab5 complex. Potential role in (S)-3,5-dihydroxyphenylglycene-induced
638 long term depression. J. Biol. Chem. 279: 12286–12292.

639 Hudmon, A., J.-S. Choi, L. Tyrrell, J. A. Black, A. M. Rush *et al.*, 2008 Phosphorylation
640 of Sodium Channel Nav1.8 by p38 Mitogen-Activated Protein Kinase Increases
641 Current Density in Dorsal Root Ganglion Neurons. J. Neurosci. 28: 3190–3201.

642 Jantsch-Plunger, V., P. Gönczy, A. Romano, H. Schnabel, D. Hamill *et al.*, 2000 CYK-4:
643 A Rho family gtpase activating protein (GAP) required for central spindle
644 formation and cytokinesis. J. Cell Biol. 149: 1391–1404.

645 Kawasaki, M., 1999 A Caenorhabditis elegans JNK signal transduction pathway
646 regulates coordinated movement via type-D GABAergic motor neurons. EMBO J.
647 18: 3604–3615.

648 Kim, D. H., R. Feinbaum, G. Alloing, F. E. Emerson, D. A. Garsin *et al.*, 2002 A
649 Conserved p38 MAP Kinase Pathway in Caenorhabditis elegans Innate
650 Immunity. Science 297: 623–626.

651 Kim, D. H., N. T. Liberati, T. Mizuno, H. Inoue, N. Hisamoto *et al.*, 2004 Integration of
652 Caenorhabditis elegans MAPK pathways mediating immunity and stress
653 resistance by MEK-1 MAPK kinase and VHP-1 MAPK phosphatase. Proc. Natl.
654 Acad. Sci. U. S. A. 101: 10990–10994.

655 Koelle, M. R., 2016 Neurotransmitter signaling through heterotrimeric G proteins:
656 insights from studies in C. elegans. WormBook, doi:10.1895/wormbook.1.75.2.

657 Kyriakis, J. M., and J. Avruch, 2012 Mammalian MAPK signal transduction pathways
658 activated by stress and inflammation: a 10-year update. Physiol. Rev. 92: 689–
659 737.

660 Lackner, M. R., S. J. Nurrish, and J. M. Kaplan, 1999 Facilitation of synaptic
661 transmission by EGL-30 Gqalpha and EGL-8 PLCbeta: DAG binding to UNC-13
662 is required to stimulate acetylcholine release. Neuron 24: 335–346.

663 Lu, B., Y. Su, S. Das, J. Liu, J. Xia *et al.*, 2007 The Neuronal Channel NALCN
664 Contributes Resting Sodium Permeability and Is Required for Normal Respiratory
665 Rhythm. Cell 129: 371–383.

McMullan, R., E. Hiley, P. Morrison, and S. J. Nurrish, 2006 Rho is a presynaptic activator of neurotransmitter release at pre-existing synapses in C. elegans. Genes Dev. 20: 65–76.

Mello, C. C., J. M. Kramer, D. Stinchcomb, and V. Ambros, 1991 Efficient gene transfer in C.elegans: extrachromosomal maintenance and integration of transforming sequences. EMBO J. 10: 3959–3970.

Miller, K. G., M. D. Emerson, and J. B. Rand, 1999 Goalpha and diacylglycerol kinase negatively regulate the Gqalpha pathway in C. elegans. Neuron 24: 323–333.

Nash, H. A., R. L. Scott, B. C. Lear, and R. Allada, 2002 An unusual cation channel mediates photic control of locomotion in Drosophila. Curr. Biol. 12: 2152–2158.

Natochin, M., and N. O. Artemyev, 2003 A point mutation uncouples transducin-alpha from the photoreceptor RGS and effector proteins. J. Neurochem. 87: 1262–1271.

Nurrish, S., L. Ségalat, and J. M. Kaplan, 1999 Serotonin inhibition of synaptic transmission: Galpha(0) decreases the abundance of UNC-13 at release sites. Neuron 24: 231–242.

Pagano, D. J., E. R. Kingston, and D. H. Kim, 2015 Tissue Expression Pattern of PMK-2 p38 MAPK Is Established by the miR-58 Family in C. elegans. PLoS Genet 11: e1004997.

685 Park, E. C., and C. Rongo, 2016 The p38 MAP kinase pathway modulates the hypoxia
686 response and glutamate receptor trafficking in aging neurons. eLife 5: e12010.

687 Plowman, G. D., S. Sudarsanam, J. Bingham, D. Whyte, and T. Hunter, 1999 The
688 protein kinases of Caenorhabditis elegans: a model for signal transduction in
689 multicellular organisms. Proc. Natl. Acad. Sci. U. S. A. 96: 13603–13610.

690 Rhee, S. G., 2001 Regulation of Phosphoinositide-Specific Phospholipase C. Annu.
691 Rev. Biochem. 70: 281–312.

692 Rush, A. M., J. Wu, M. J. Rowan, and R. Anwyl, 2002 Group I metabotropic glutamate
693 receptor (mGluR)-dependent long-term depression mediated via p38 mitogen-
694 activated protein kinase is inhibited by previous high-frequency stimulation and
695 activation of mGluRs and protein kinase C in the rat dentate gyrus in vitro. J.
696 Neurosci. 22: 6121–6128.

697 Sagasti, A., N. Hisamoto, J. Hyodo, M. Tanaka-Hino, K. Matsumoto *et al.*, 2001 The
698 CaMKII UNC-43 Activates the MAPKKK NSY-1 to Execute a Lateral Signaling
699 Decision Required for Asymmetric Olfactory Neuron Fates. Cell 105: 221–232.

700 Sánchez-Fernández, G., S. Cabezudo, C. García-Hoz, C. Benincá, A. M. Aragay *et al.*,
701 2014 Gαq signalling: The new and the old. Cell. Signal. 26: 833–848.

702 Shi, Y., C. Abe, B. B. Holloway, S. Shu, N. N. Kumar *et al.*, 2016 Nalcn Is a “Leak”
703 Sodium Channel That Regulates Excitability of Brainstem Chemosensory
704 Neurons and Breathing. J. Neurosci. 36: 8174–8187.

705 Shivers, R. P., T. Kooistra, S. W. Chu, D. J. Pagano, and D. H. Kim, 2009 Tissue-
706 specific activities of an immune signaling module regulate physiological
707 responses to pathogenic and nutritional bacteria in C. elegans. Cell Host Microbe
708 6: 321–330.

709 Shivers, R. P., D. J. Pagano, T. Kooistra, C. E. Richardson, K. C. Reddy *et al.*, 2010
710 Phosphorylation of the conserved transcription factor ATF-7 by PMK-1 p38
711 MAPK regulates innate immunity in Caenorhabditis elegans. PLoS Genet. 6:
712 e1000892.

713 Tanaka-Hino, M., A. Sagasti, N. Hisamoto, M. Kawasaki, S. Nakano *et al.*, 2002 SEK-1
714 MAPKK mediates Ca2+ signaling to determine neuronal asymmetric
715 development in Caenorhabditis elegans. EMBO Rep. 3: 56–62.

716 Topalidou, I., J. Cattin-Ortolá, A. L. Pappas, K. Cooper, G. E. Merrihew *et al.*, 2016 The
717 EARP Complex and Its Interactor EIPR-1 Are Required for Cargo Sorting to
718 Dense-Core Vesicles. PLOS Genet 12: e1006074.

719 Topalidou, I., P.-A. Chen, K. Cooper, S. Watanabe, E. M. Jorgensen *et al.*, 2017 The
720 NCA-1 and NCA-2 Ion Channels Function Downstream of Gq and Rho To
721 Regulate Locomotion in Caenorhabditis elegans. Genetics 206: 265–282.

722 Vaqué, J. P., R. T. Dorsam, X. Feng, R. Iglesias-Bartolome, D. J. Forsthoefel *et al.*,
723 2013 A genome-wide RNAi screen reveals a Trio-regulated Rho GTPase circuitry
724 transducing mitogenic signals initiated by G protein-coupled receptors. Mol. Cell
725 49: 94–108.

726 Vashlishan, A. B., J. M. Madison, M. Dybbs, J. Bai, D. Sieburth *et al.*, 2008 An RNAi
727 Screen Identifies Genes that Regulate GABA Synapses. Neuron 58: 346–361.

728 Williams, S. L., S. Lutz, N. K. Charlie, C. Vettel, M. Ailion *et al.*, 2007 Trio's Rho-specific
729 GEF domain is the missing Galpha q effector in C. elegans. Genes Dev. 21:
730 2731–2746.

731 Wittmack, E. K., A. M. Rush, A. Hudmon, S. G. Waxman, and S. D. Dib-Hajj, 2005
732 Voltage-Gated Sodium Channel Nav1.6 Is Modulated by p38 Mitogen-Activated
733 Protein Kinase. J. Neurosci. 25: 6621–6630.

734 Zhang, R., X. He, W. Liu, M. Lu, J.-T. Hsieh *et al.*, 2003 AIP1 mediates TNF-α–induced
735 ASK1 activation by facilitating dissociation of ASK1 from its inhibitor 14-3-3. J.
736 Clin. Invest. 111: 1933–1943.

737

Figure 1

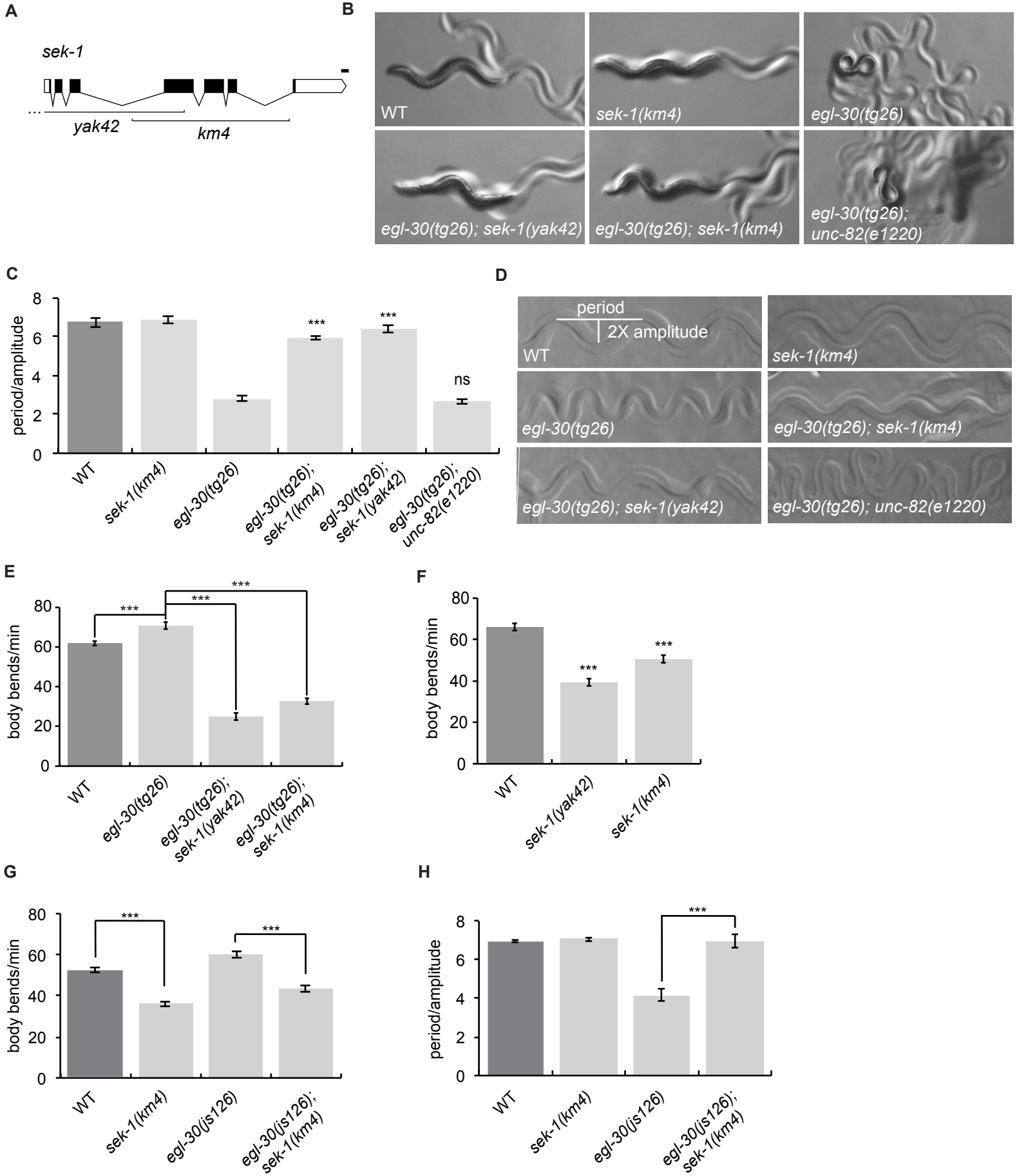

Figure 2

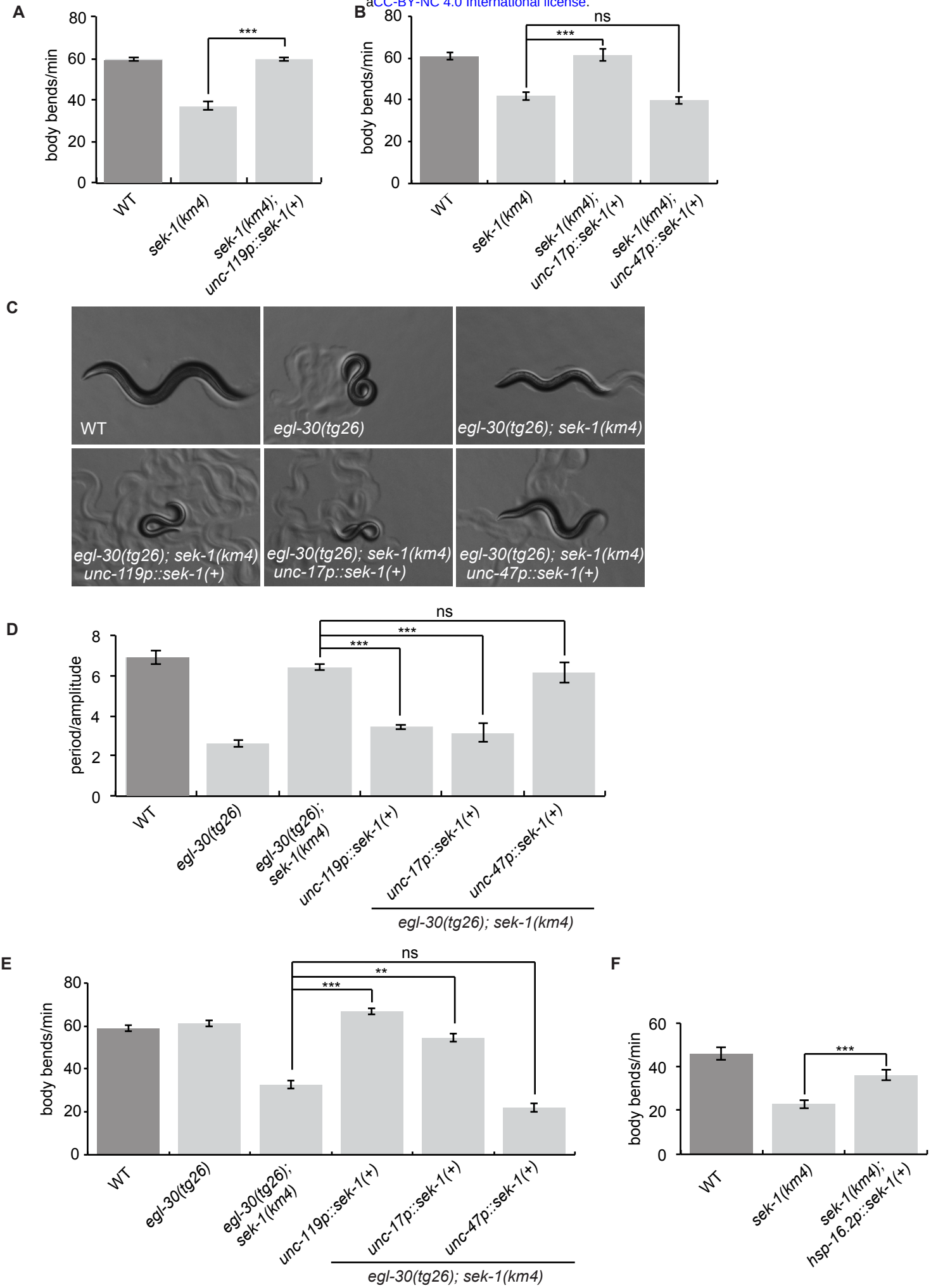

Figure 3

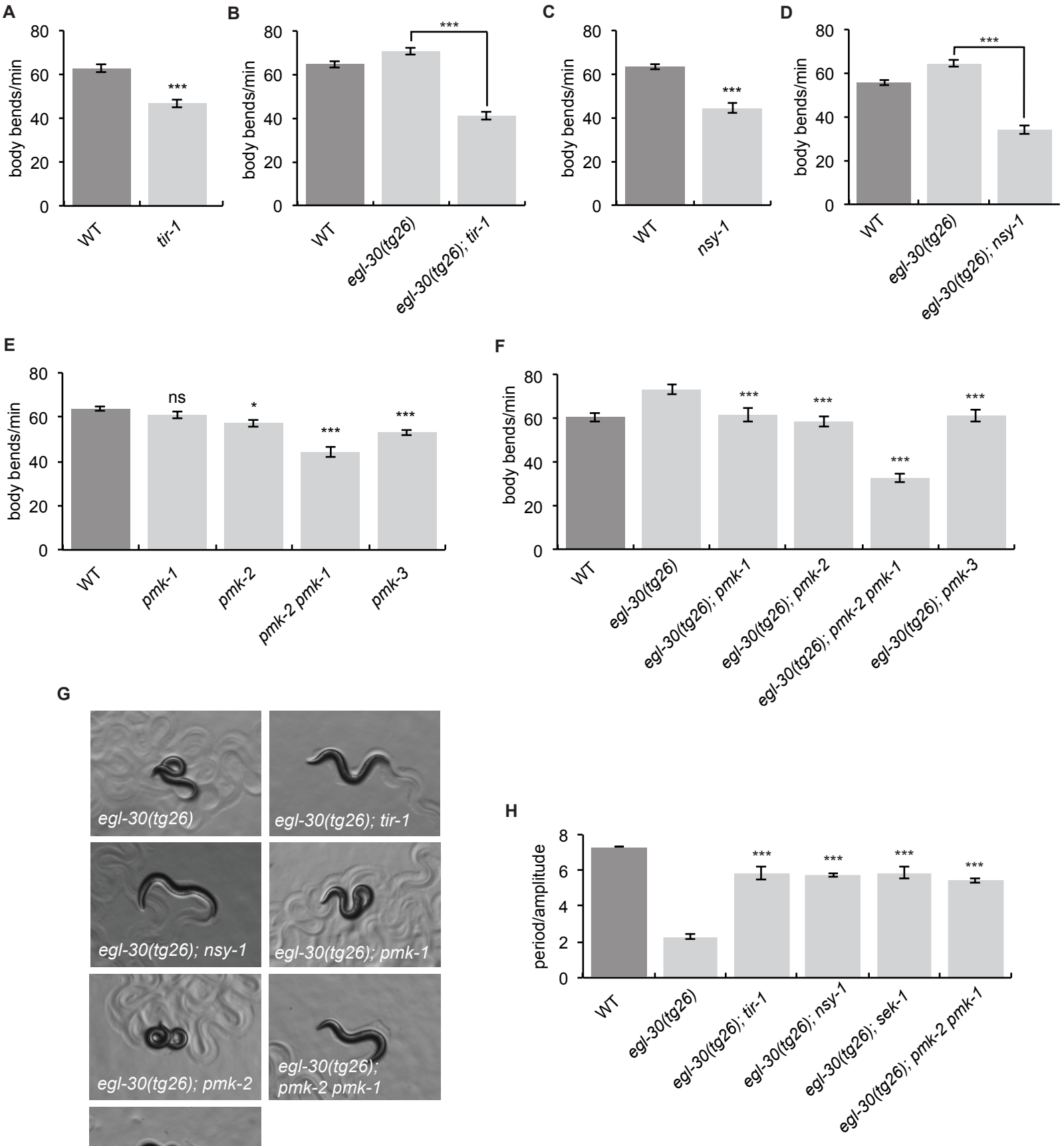

Figure 4

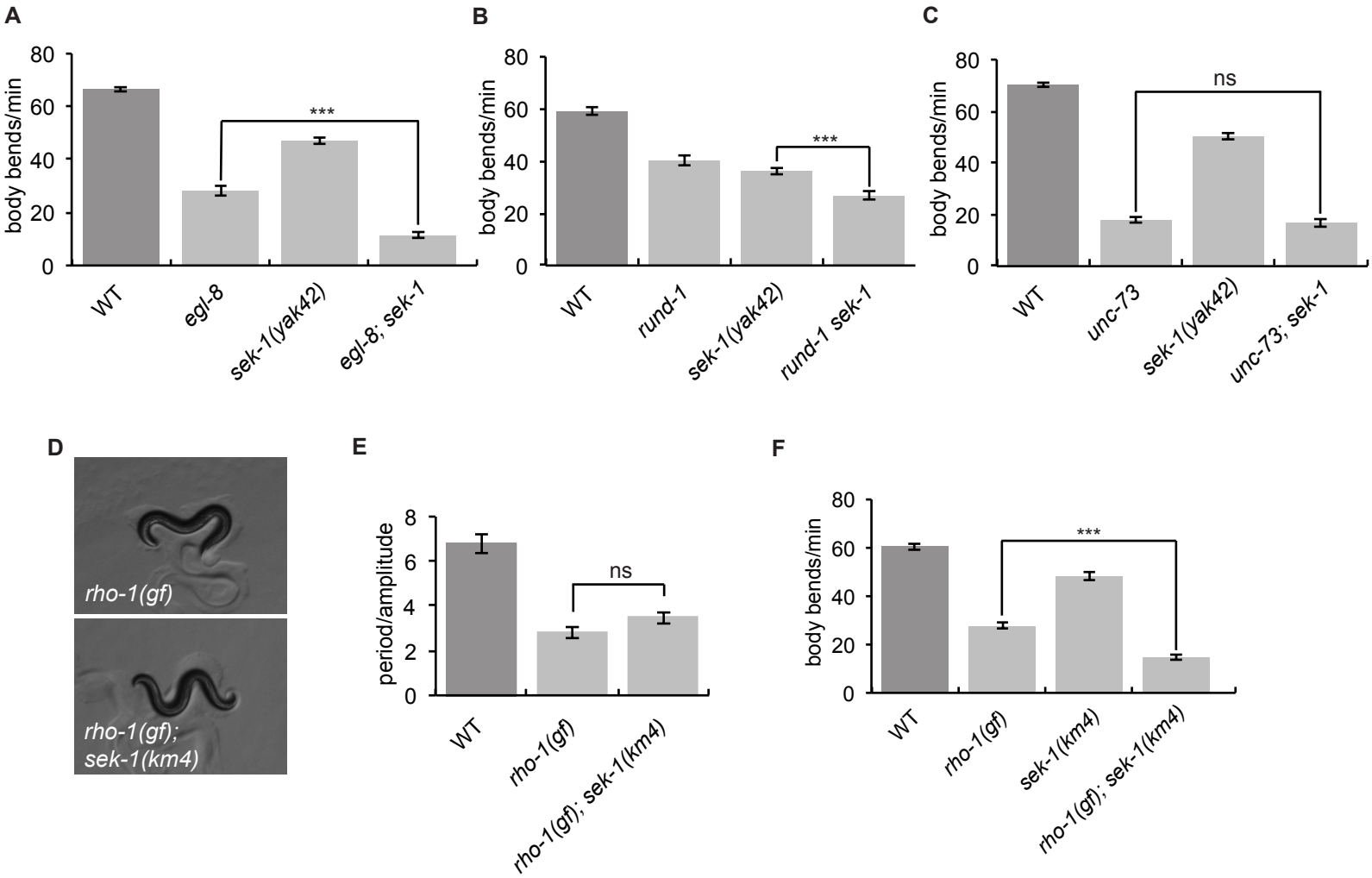

Figure 5

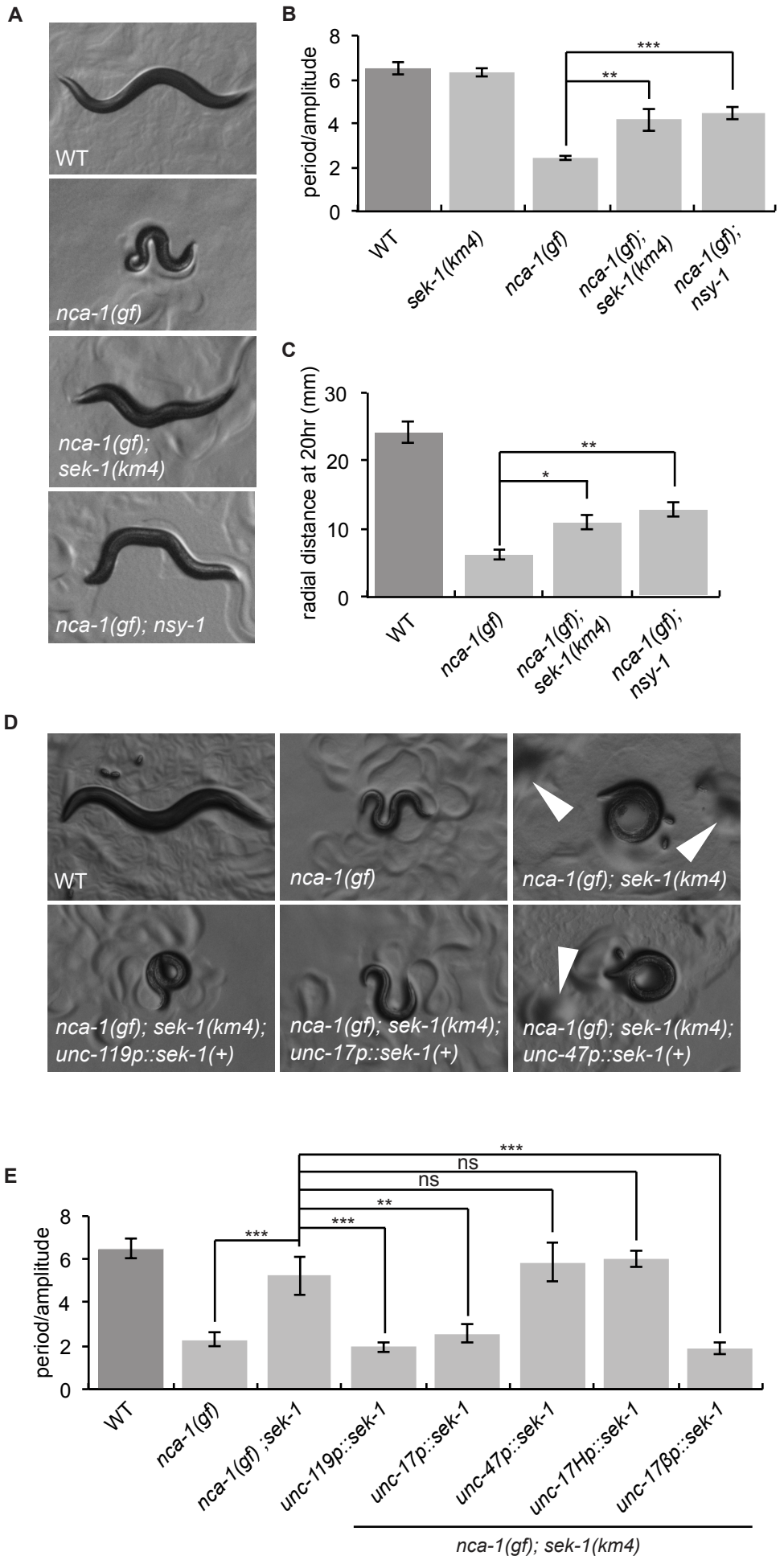

Supplementary Information

Table S1. Strain List

Strain	Genotype
AU1	*sek-1(ag1)* X
BS3383	*pmk-3(ok169)* IV
CX3695	*kyIs140[str-2p::gfp, lin-15(+)]* I
CX5959	*kyIs140[str-2p::gfp, lin-15(+)]* I; *tir-1(ky648gf)* III
EG317	*unc-73(ox317)* I
EG1000	*dpy-5(e61)* I; *rol-6(e187)* II; *lon-1(e1820)* III
EG1020	*bli-6(sc16)* IV; *dpy-11(e224)* V; *lon-2(e678)* X
EG3745	*eat-16(tm775)* I *; him-5(e1490)* V
EG4782	*nzIs29[unc-17p::rho-1(G14V), unc-122::gfp]* II
EG5505	*rund-1(tm3622)* X
EG7989	*unc-119(ed3)* III; *oxTi668[eft-3p::TdTomato::H2B, Cb-unc-119(+)]* X
IG685	*tir-1(tm3036)* III
JN147	*gap-2(tm748)* X
JT47	*egl-8(sa47)* V
JT366	*vhp-1(sa366)* II
JT734	*goa-1(sa734)* I
KU2	*jkk-1(km2)* X
KU4	*sek-1(km4)* X
KU25	*pmk-1(km25)* IV
N2	Bristol wild isolate, standard lab wild-type
NM1380	*egl-30(js126gf)* I

VC8	*jnk-1(gk7)* IV
VC390	*nsy-1(ok593)* IV
XZ42	*sek-1(yak42)* X
XZ1233	*egl-30(tg26)* I*; sek-1(yak42)* X
XZ1151	*egl-30(tg26)* I
XZ1566	*egl-8(sa47)* V*; sek-1(yak42)* X
XZ1567	*unc-73(ox317)* I*; sek-1(yak42)* X
XZ1574	*rund-1(tm3622) sek-1(yak42)* X
XZ1575	*egl-30(tg26)* I*; sek-1(km4)* X
XZ1588	*egl-30(tg26)* I*; nsy-1(ok593)* IV
XZ1589	*egl-30(tg26)* I*; sek-1(km4)* X*; qdEx8[unc-119p::sek-1::GFP, myo-2p::mStrawberry::unc-54-3'UTR]*
XZ1590	*egl-30(tg26)* I *; jkk-1(km2)* X
XZ1593	*egl-30(tg26)* I*; pmk-1(km25)* IV
XZ1597	*egl-30(tg26)* I *; jnk-1(gk7)* IV
XZ1642	*sek-1(km4)* X*; yakEx72[unc-17p::sek-1::tbb-2utr-operon-GFP::H2B::cye-1utr, myo-2p::mCherry]*
XZ1643	*sek-1(km4)* X*; yakEx73[unc-47p::sek-1::tbb-2utr-operon-GFP::H2B::cye-1utr, myo-2p::mCherry]*
XZ1717	*nzIs29[unc-17p::rho-1(G14V) unc-122::gfp]* II*; sek-1(km4)* X
XZ1720	*sek-1(km4)* X *; yakEx82[unc-17Hp::sek-1:: tbb-2utr-operon-GFP::H2B::cye-1utr, myo-2p::mCherry]*
XZ1721	*sek-1(km4)* X *; yakEx83[unc-17βp::sek-1::tbb-2utr-operon-GFP::H2B::cye-1utr, myo-2p::mCherry]*
XZ1770	*egl-30(tg26)* I*; pmk-2(qd279 qd171) pmk-1(km25)* IV

XZ1771	*egl-30(tg26)* I*; pmk-2(qd287)* IV
XZ1772	*egl-30(tg26)* I*; pmk-3(ok169)* IV
XZ1815	*egl-30(tg26)* I*; tir-1(tm3036)* III
XZ1816	*nca-1(ox352)* IV*; sek-1(km4)* X*; qdEx8[unc-119p::sek-1::GFP::unc-54-3' UTR, myo-2p::mStrawberry::unc-54-3'UTR]*
XZ1820	*nca-1(ox352)* IV *; sek-1(km4)* X *; yakEx83[unc-17βp::sek-1::tbb-2utr-operon-GFP::H2B::cye-1utr, myo-2p::mCherry]*
XZ1830	*egl-30(tg26)* I *; sek-1(km4)* X *; yakEx83[unc-17βp::sek-1::tbb-2utr-operon-GFP::H2B::cye-1utr, myo-2p::mCherry]*
XZ1834	*egl-30(tg26)* I*; sek-1(km4)* X*; yakEx72[unc-17p::sek-1::tbb-2utr-operon-GFP::H2B::cye-1utr, myo-2p::mCherry]*
XZ1835	*nca-1(ox352)* IV*; sek-1(km4)* X*; yakEx72[unc-17p::sek-1::tbb-2utr-operon-GFP::H2B::cye-1utr, myo-2p::mCherry]*
XZ1861	*nca-1(ox352)* IV*; sek-1(km4)* X*; yakEx73[unc-47p::sek-1::tbb-2utr-operon-GFP::H2B::cye-1utr, myo-2p::mCherry]*
XZ1862	*nca-1(ox352)* IV *; sek-1(km4)* X *; yakEx82[unc-17Hp::sek-1::tbb-2utr-operon-GFP::H2B::cye-1utr, myo-2p::mCherry]*
XZ1863	*egl-30(tg26)* I*; sek-1(km4)* X*; yakEx73[unc-47p::sek-1::tbb-2utr-operon-GFP::H2B::cye-1utr, myo-2p::mCherry]*
XZ1872	*jnk-1(gk7)* I*; sek-1(km4)* X
XZ1873	*pmk-2(qd279 qd171) pmk-1(km25)* IV*; jkk-1(km2)* X
XZ1879	*egl-30(tg26)* I *; sek-1(km4)* X *; yakEx82[unc-17Hp:: sek-1::tbb-2utr-operon-GFP::H2B::cye-1utr, myo-2p::mCherry]*
XZ1902	*egl-30(tg26)* I *; unc-82(e1220)* IV
XZ1937	*sek-1(km4)* X*; yakEx121[hsp-16.2p::sek-1::tbb-2-3' UTR::gld-1 operon*

	linker::gfp::h2b, myo-2p::mCherry]
XZ1938	*egl-30(tg26)* I *; agIs219[T24B8.5p::GFP::unc-54-3'UTR + ttx-3p::GFP::unc-54-3'UTR]* III *atf-7(qd22 qd130)* III
XZ1939	*goa-1(sa734)* I*; sek-1(km4)* X
XZ1942	*tir-1(ky648gf)* III
XZ2054	*eat-16(tm775)* I *; sek-1(km4)* X
XZ2062	*egl-30(js126gf)* I *; sek-1(km4)* X
ZD202	*sek-1(km4)* X*; qdEx8[unc-119p::sek-1::GFP::unc-54-3' UTR + myo-2p::mStrawberry::unc-54-3'UTR]*
ZD318	*agIs29 atf-7(qd22 qd130)* III
ZD442	*agIs29 atf-7(qd22)* III
ZD934	*pmk-2(qd279 qd171) pmk-1(km25)* IV
ZD1020	*pmk-2(qd287)* IV

Table S2. Plasmids and Primers

Gateway entry clones

Plasmid	Details
pADA180	*unc-17Hp* [4-1]
pJH21	*sek-1* cDNA [1-2]
pCFJ150	pDEST5605[4-3]
pCFJ326	*tbb-2utr-operon-GFP::H2B::cye-1utr* [2-3]
pMA23	*unc-17βp* [4-1]
pMH522	*unc-47p* [4-1]
pGH1	*unc-17p* [4-1]
pCM1.56	*hsp-16.2p* [4-1]

Gateway Expression Constructs

Plasmid	Details	Used to make
pJH23	*unc-17p::sek-1::tbb-2utr-operon-GFP::H2B::cye-1utr*	*yakEx72*
pJH24	*unc-47p::sek-1::tbb-2utr-operon-GFP::H2B::cye-1utr*	*yakEx73*
pJH28	*unc-17Hp::sek-1::tbb-2utr-operon-GFP::H2B::cye-1utr*	*yakEx82*
pJH29	*unc-17βp::sek-1::tbb-2utr-operon-GFP::H2B::cye-1utr*	*yakEx83*
pJH46	*hsp-16.2p::sek-1::tbb-2utr-operon-GFP::H2B::cye-1utr*	*yakEx121*

Primers

oJH114	GGGGACAAGTTTGTACAAAAAAGCAGGCTcaATGGAGCGAAAAGGACGTG	F to clone *sek-1* cDNA into [1-2]
oJH115	GGGGACCACTTTGTACAAGAAAGCTGGGTgTCATCGTCGCCAAACAGTG	R to clone *sek-1* cDNA into [1-2]

Table S3. Statistical Tests

Figure	Test	p value
1C	One-way ANOVA and Bonferroni's Multiple Comparison Test WT vs *sek-1(km4)* (ns)	< 0.001

	WT vs *egl-30(tg26)* (p<0.001) *egl-30(tg26)* vs *egl-30(tg26); sek-1(km4)* (p<0.001) *egl-30(tg26)* vs *egl-30(tg26); sek-1(yak42)* (p<0.001) *egl-30(tg26)* vs *egl-30(tg26); unc-82(e1220)* (ns)	
1E	One-way ANOVA and Bonferroni's Multiple Comparison Test WT vs *egl-30(tg26)* (p<0.001) *egl-30(tg26)* vs *egl-30(tg26); sek-1(yak42)* (p<0.001) *egl-30(tg26)* vs *egl-30(tg26); sek-1(km4)* (p<0.001)	< 0.001
1F	One-way ANOVA and Dunnett's Multiple Comparison Test WT vs *sek-1(yak42)* (p<0.001) WT vs *sek-1(km4)* (p<0.001)	< 0.001
1G	One-way ANOVA and Bonferroni's Multiple Comparison Test WT vs *egl-30(js126)* (p<0.001) WT vs *sek-1(km4)* (p<0.001) *egl-30(js126)* vs *egl-30(js126); sek-1(km4)* (p<0.001)	< 0.001
1H	One-way ANOVA and Bonferroni's Multiple Comparison Test WT vs *egl-30(js126)* (p<0.001) *egl-30(js126)* vs *egl-30(js126); sek-1(km4)* (p<0.001)	<0.001
2A	One-way ANOVA and Bonferroni's Multiple Comparison Test *sek-1(km4)* vs *sek-1(km4); qdEx8[unc-119::sek-1(+)]* (p<0.001)	< 0.001
2B	One-way ANOVA and Bonferroni's Multiple Comparison Test *sek-1(km4)* vs *sek-1(km4); yakEx72[unc-17p::sek-1(+)]* (p<0.001) *sek-1(km4)* vs *sek-1(km4); yakEx73[unc-47p::sek-1(+)]* (ns)	<0.001
2D	One-way ANOVA and Bonferroni's Multiple Comparison Test WT vs *egl-30(tg26)* (p<0.001)	<0.001

	egl-30(tg26); sek-1(km4) vs *egl-30(tg26); sek-1(km4); qdEx8[unc-119p::sek-1(+)]* (p<0.001) *egl-30(tg26); sek-1(km4)* vs *egl-30(tg26); sek-1(km4); yakEx72[unc-17p::sek-1(+)]* (p<0.001) *egl-30(tg26); sek-1(km4)* vs *egl-30(tg26); sek-1(km4); yakEx73[unc-47p::sek-1(+)]* (ns)	
2E	Kruskal-Wallis Test and Dunn's Multiple Comparison Test *egl-30(tg26); sek-1(km4)* vs *egl-30(tg26); sek-1(km4); qdEx8[unc-119p::sek-1(+)]* (p<0.001) *egl-30(tg26); sek-1(km4)* vs *egl-30(tg26); sek-1(km4); yakEx72[unc-17p::sek-1(+)]* (p<0.01) *egl-30(tg26); sek-1(km4)* vs *egl-30(tg26); sek-1(km4); yakEx73[unc-47p::sek-1(+)]* (ns)	< 0.001
2F	One-way ANOVA and Bonferroni's Multiple Comparison Test *sek-1(km4)* vs *sek-1(km4); yakEx121[hsp-16.2p::sek-1(+)]* (p<0.001)	< 0.001
3A	Unpaired t test, two-tailed	< 0.001
3B	One-way ANOVA and Bonferroni's Multiple Comparison Test *egl-30(tg26)* vs *egl-30(tg26); tir-1(tm3036)* (p<0.001)	< 0.001
3C	Unpaired t test, two-tailed	< 0.001
3D	One-way ANOVA and Bonferroni's Multiple Comparison Test *egl-30(tg26)* vs *egl-30(tg26); nsy-1(ok593)* (p<0.001)	< 0.001
3E	One-way ANOVA and Dunnett's Multiple Comparison Test	< 0.001

	WT vs *pmk-1(km25)* (ns) WT vs *pmk-2(qd287)* (p<0.05) WT vs *pmk-2(qd279 qd171) pmk-1 (km25)* (p<0.001) WT vs *pmk-3(ok169)* (p<0.001)	
3F	One-way ANOVA and Dunnett's Multiple Comparison Test *egl-30(tg26)* vs *egl-30(tg26); pmk-1(km25)* (p<0.001) *egl-30(tg26)* vs *egl-30(tg26); pmk-2(qd287)* (p<0.001) *egl-30(tg26)* vs *egl-30(tg26); pmk-2(qd279 qd171) pmk-1 (km25)* (p<0.001) *egl-30(tg26)* vs *egl-30(tg26); pmk-3(ok169)* (p<0.001)	< 0.001
3H	One-way ANOVA and Bonferroni's Multiple Comparison Test *egl-30(tg26)* vs *egl-30(tg26); tir-1(tm3036)* (p<0.001) *egl-30(tg26)* vs *egl-30(tg26); nsy-1(ok593)* (p<0.001) *egl-30(tg26)* vs *egl-30(tg26); sek-1(km4)* (p<0.001) *egl-30(tg26)* vs *egl-30(tg26); pmk-2(qd279 qd171) pmk-1(km25)* (p<0.001)	< 0.001
4A	One-way ANOVA and Bonferroni's Multiple Comparison Test *egl-8(sa47)* vs *egl-8(sa47); sek-1(yak42)* (p<0.001)	< 0.001
4B	One-way ANOVA and Bonferroni's Multiple Comparison Test *sek-1(yak42)* vs *rund-1(tm3622); sek-1(yak42)* (p<0.001)	< 0.001
4C	One-way ANOVA and Bonferroni's Multiple Comparison Test *unc-73(ox317)* vs *unc-73(ox317); sek-1(yak42)* (ns)	< 0.001
4E	One-way ANOVA and Bonferroni's Multiple Comparison Test WT vs *nzIs29[unc-17p::rho-1(G14V)]* (p<0.001) WT vs *nzIs29[unc-17p::rho-1(G14V)]; sek-1(km4)* (p<0.001)	< 0.001

	nzIs29[unc-17p::rho-1(G14V)] vs *nzIs29[unc-17p::rho-1(G14V)]; sek-1(km4)* (ns)	
4F	One-way ANOVA and Bonferroni's Multiple Comparison Test *nzIs29[unc-17p::rho-1(G14V)]* vs *nzIs29[unc-17p::rho-1(G14V)]; sek-1(km4)* (p<0.001)	< 0.001
5B	One-way ANOVA and Bonferroni's Multiple Comparison Test WT vs *sek-1(km4)* (ns) WT vs *nca-1(ox352)* (p<0.001) *nca-1(ox352)* vs *nca-1(ox352); sek-1(km4)* (p<0.01) *nca-1(ox352)* vs *nca-1(ox352); nsy-1(ok593)* (p<0.001)	<0.001
5C	One-way ANOVA and Bonferroni's Multiple Comparison Test WT vs *nca-1(ox352)* (p<0.001) *nca-1(ox352)* vs *nca-1(ox352); nsy-1(ok593)* (p<0.01) *nca-1(ox352)* vs *nca-1(ox352); sek-1(km4)* (p<0.05)	< 0.001
5E	One-way ANOVA and Bonferroni's Multiple Comparison Test *nca-1(ox352)* vs *nca-1(ox352); sek-1(km4)* (p<0.001) *nca-1(ox352); sek-1(km4)* vs *nca-1(ox352); sek-1(km4); qdEx8[unc-119p::sek-1(+)]* (p<0.001) *nca-1(ox352); sek-1(km4)* vs *nca-1(ox352); sek-1(km4); yakEx72[unc-17p::sek-1(+)]* (p<0.01) *nca-1(ox352); sek-1(km4)* vs *nca-1(ox352); sek-1(km4); yakEx73[unc-47p::sek-1(+)]* (ns) *nca-1(ox352); sek-1(km4)* vs	< 0.001

	nca-1(ox352); sek-1(km4); yakEx82[unc-17Hp::sek-1(+)] (ns) *nca-1(ox352); sek-1(km4)* vs *nca-1(ox352); sek-1(km4); yakEx83[unc-17βp::sek-1(+)]* ($p<0.001$)	
S1A	One-way ANOVA and Bonferroni's Multiple Comparison Test WT vs *egl-30(tg26)* ($p<0.01$) WT vs *sek-1(km4)* ($p<0.001$) *egl-30(tg26)* vs *egl-30(tg26); sek-1(km4)* ($p<0.001$) *sek-1(km4)* vs *egl-30(tg26); sek-1(km4)* ($p<0.01$)	< 0.001
S1B	One-way ANOVA and Newman-Keuls Multiple Comparison Test WT vs *sek-1(yak42)* ($p<0.001$) WT vs *sek-1(ag1)* ($p<0.001$) *sek-1(yak42)* vs *sek-1(ag1)* (ns)	< 0.001
S1C	One-way ANOVA and Bonferroni's Multiple Comparison Test WT vs *egl-30(tg26)* (ns) *egl-30(tg26)* vs *egl-30(tg26); unc-82(e1220)* ($p<0.001$)	< 0.001
S1D	One-way ANOVA and Bonferroni's Multiple Comparison Test WT vs *sek-1(km4)* ($p<0.001$) *goa-1(sa734)* vs *sek-1(km4)* ($p<0.001$) *goa-1(sa734)* vs *goa-1(sa734); sek-1(km4)* ($p<0.001$)	< 0.001
S1E	One-way ANOVA and Bonferroni's Multiple Comparison Test WT vs *sek-1(km4)* (ns) WT vs *goa-1(sa734)* ($p<0.001$) *goa-1(sa734)* vs *goa-1(sa734); sek-1(km4)* ($p<0.001$)	< 0.001
S1F	One-way ANOVA and Bonferroni's Multiple Comparison Test	< 0.001

	WT vs *sek-1(km4)* (p<0.001) WT vs *eat-16(tm775)* (p<0.001) *eat-16(tm775)* vs *eat-16(tm775); sek-1(km4)* (p<0.001) *sek-1(km4) vs eat-16(tm775); sek-1(km4)* (ns)	
S1G	One-way ANOVA and Bonferroni's Multiple Comparison Test WT vs *eat-16(tm775)* (p<0.001) *eat-16(tm775)* vs *eat-16(tm775); sek-1(km4)* (ns)	< 0.001
S2A	One-way ANOVA and Bonferroni's Multiple Comparison Test WT vs *sek-1(km4)* (p<0.001) *sek-1(km4)* vs *sek-1(km4); yakEx82[unc-17Hp::sek-1(+)]* (p<0.05) *sek-1(km4)* vs *sek-1(km4); yakEx83[unc-17βp::sek-1(+)]* (p<0.01)	< 0.001
S2B	One-way ANOVA and Bonferroni's Multiple Comparison Test *egl-30(tg26); sek-1(km4)* vs *egl-30(tg26); sek-1(km4); yakEx82[unc-17Hp::sek-1(+)]* (p<0.001) *egl-30(tg26); sek-1(km4)* vs *egl-30(tg26); sek-1(km4); yakEx83[unc-17βp::sek-1(+)]* (p<0.001)	< 0.001
S2C	One-way ANOVA and Bonferroni's Multiple Comparison Test WT vs *egl-30(tg26)* (p<0.001) *egl-30(tg26); sek-1(km4)* vs *egl-30(tg26); sek-1(km4); qdEx8[unc-119p::sek-1(+)]* (p<0.001) *egl-30(tg26); sek-1(km4)* vs *egl-30(tg26); sek-1(km4); yakEx72[unc-17p::sek-1(+)]* (p<0.001) *egl-30(tg26); sek-1(km4)* vs	< 0.001

	egl-30(tg26); sek-1(km4); yakEx73[unc-47p::sek-1(+)] (ns) *egl-30(tg26); sek-1(km4)* vs *egl-30(tg26); sek-1(km4); yakEx82[unc-17Hp::sek-1(+)]* (p<0.001) *egl-30(tg26); sek-1(km4)* vs *egl-30(tg26); sek-1(km4); yakEx83[unc-17βp::sek-1(+)]* (ns)	
S3A	One-way ANOVA and Bonferroni's Multiple Comparison Test *jnk-1(gk7)* vs *jnk-1(gk7); sek-1(km4)* (p<0.01) *jkk-1(km2) vs pmk-2(qd279 qd171) pmk-1 (km25); jkk-1(km2)* (p<0.05)	< 0.05
S3B	One-way ANOVA and Bonferroni's Multiple Comparison Test WT vs *egl-30(tg26)* (P<0.001) *egl-30(tg26)* vs *egl-30(tg26)*; *jkk-1* (ns) *egl-30(tg26)* vs *egl-30(tg26)*; *jnk-1* (ns) *egl-30(tg26)* vs *egl-30(tg26)*; *atf-7* (ns)	
S3C	One-way ANOVA and Bonferroni's Multiple Comparison Test WT vs *atf-7(qd22)* (p<0.001) WT vs *atf-7(qd22 qd130)* (p<0.001)	< 0.001
S3D	One-way ANOVA	p=0.806
S3F	Unpaired t test, two-tailed	< 0.001
S4A	One-way ANOVA and Bonferroni's Multiple Comparison Test WT vs *nca-1(ox352)* (p<0.001) *nca-1(ox352)* vs *nca-1(ox352); sek-1(km4)* (p<0.001) *nca-1(ox352)* vs *nca-1(ox352); nsy-1(ok593)* (p<0.001)	<0.001
S4B	Kruskal-Wallis Test and Dunn's Multiple Comparison Test	0.001

	nca-1(ox352);sek-1(km4) vs *nca-1(ox352);sek-1(km4); qdEx8[unc-119p::sek-1(+)]* (ns) *nca-1(ox352);sek-1(km4)* vs *nca-1(ox352);sek-1(km4); yakEx72[unc-17p::sek-1(+)]* (ns) *nca-1(ox352);sek-1(km4)* vs *nca-1(ox352);sek-1(km4); yakEx73[unc-47p::sek-1(+)]* (ns)	
S4C	One-way ANOVA and Bonferroni's Multiple Comparison Test *nca-1(ox352)* vs *nca-1(ox352); sek-1(km4)* (p<0.001) *nca-1(ox352); sek-1(km4)* vs *nca-1(ox352); sek-1(km4); qdEx8[unc-119p::sek-1(+)]* (p<0.001) *nca-1(ox352); sek-1(km4)* vs *nca-1(ox352); sek-1(km4); yakEx72[unc-17p::sek-1(+)]* (p<0.001) *nca-1(ox352); sek-1(km4)* vs *nca-1(ox352); sek-1(km4); yakEx73[unc-47p::sek-1(+)]* (ns) *nca-1(ox352); sek-1(km4)* vs *nca-1(ox352); sek-1(km4); yakEx82[unc-17Hp::sek-1(+)]* (p<0.001) *nca-1(ox352); sek-1(km4)* vs *nca-1(ox352); sek-1(km4); yakEx83[unc-17βp::sek-1(+)]* (p<0.001)	<0.001

Figure S1

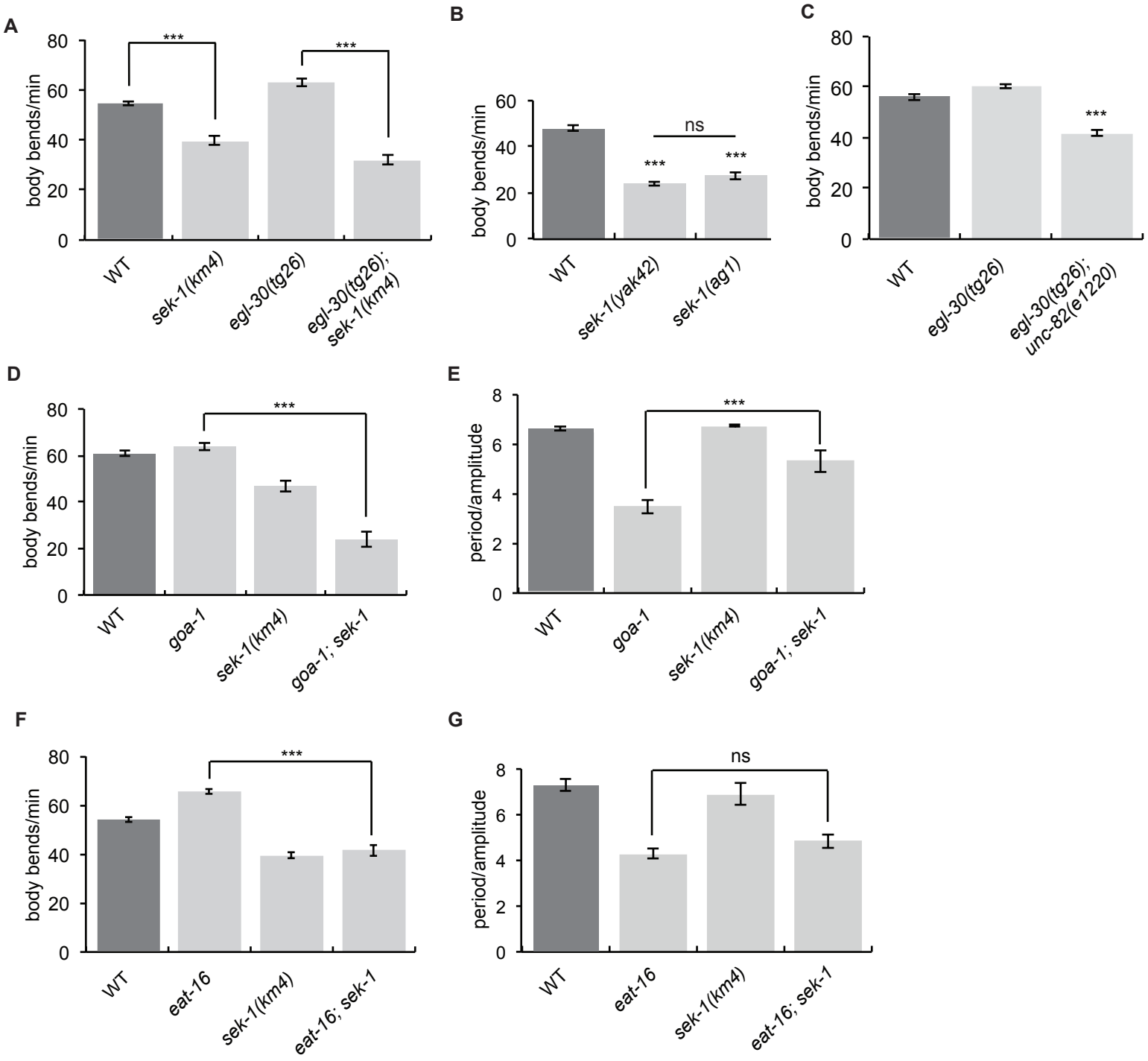

Figure S1. *sek-1* interacts with Gq and Go mutants

(A) The *sek-1(km4)* mutation suppresses the hyperactive locomotion of the activated Gq mutant *egl-30(tg26)*. ***, p<0.001, error bars = SEM, n=20.

(B) *sek-1(ag1)* mutant animals have slow locomotion. ***, p<0.001, error bars = SEM, n=10.

(C) The *unc-82(e1220)* mutation reduces the locomotion rate of the activated Gq mutant *egl-30(tg26).* ***, p<0.001, error bars = SEM, n= 20.

(D) *sek-1(km4)* suppresses the hyperactivity of *goa-1(sa734).* ***, p<0.001, error bars = SEM, n=20.

(E) *sek-1(km4)* suppresses the loopy waveform of *goa-1(sa734)*. ***, p<0.001, error bars = SEM, n=5.

(F) *sek-1(km4)* suppresses the hyperactivity of *eat-16(tm775).* ***, p<0.001, error bars = SEM, n=20.

(G) *sek-1(km4)* does not suppress the loopy waveform of *eat-16(tm775).* ns, p>0.05, error bars = SEM, n=5.

Figure S2

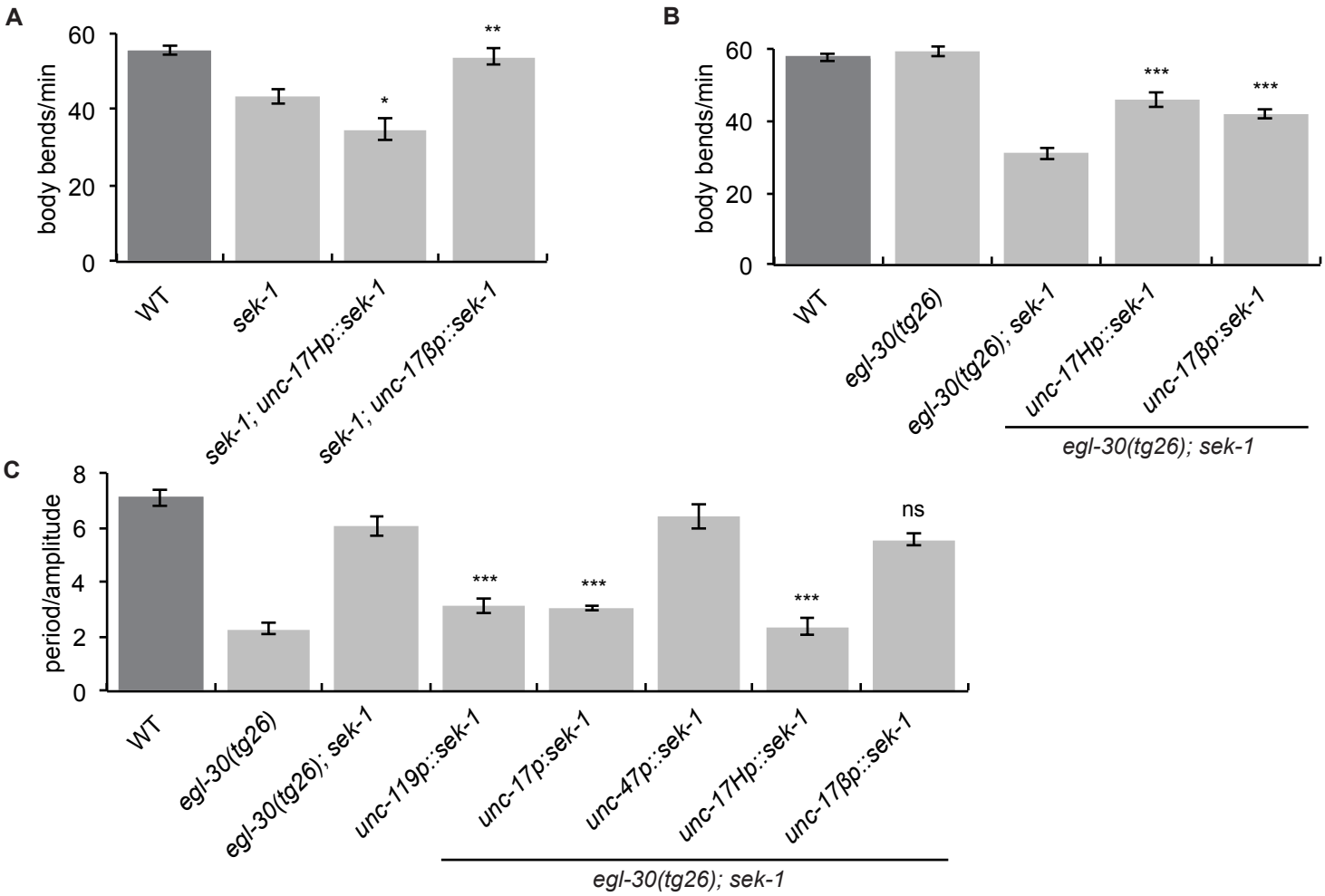

Figure S2. *sek-1* acts in both head acetylcholine neurons and acetylcholine motorneurons
(A) *sek-1* acts in acetylcholine motorneurons to modulate locomotion rate. The *sek-1* WT cDNA driven by the *unc-17β* acetylcholine motorneuron promoter [*unc-17βp::sek-1(+)*] rescues the slow locomotion phenotype of *sek-1(km4)* worms, but *sek-1* expression in head acetylcholine neurons using the *unc-17H* promoter [*unc-17Hp::sek-1(+)*] does not rescue. **, p< 0.01; *, p<0.05 compared to *sek-1*. Error bars = SEM, n=20.
(B) *sek-1* acts in both head acetylcholine neurons and acetylcholine motorneurons to modulate the locomotion rate of the activated Gq mutant *egl-30(tg26). egl-30(tg26) sek-1(km4)* worms expressing either *unc-17Hp::sek-1(+)* or *unc-17βp::sek-1(+)* have an increased locomotion rate compared to *egl-30(tg26) sek-1.* ***, p<0.001 compared to *egl-30(tg26) sek-1.* Error bars = SEM, n=20.
(C) *sek-1* acts in head acetylcholine neurons to modulate the loopy waveform of the activated Gq mutant *egl-30(tg26)*. *egl-30(tg26) sek-1(km4)* worms expressing *unc-17Hp::sek-1(+)* are loopy like *egl-30(tg26)*, but *egl-30(tg26) sek-1(km4*) worms expressing *unc-17βp::sek-1(+)* are similar to *egl-30(tg26) sek-1.* ***, p<0.001; ns, p>0.05 compared to *egl-30(tg26) sek-1*. Error bars = SEM, n=5.

Figure S3

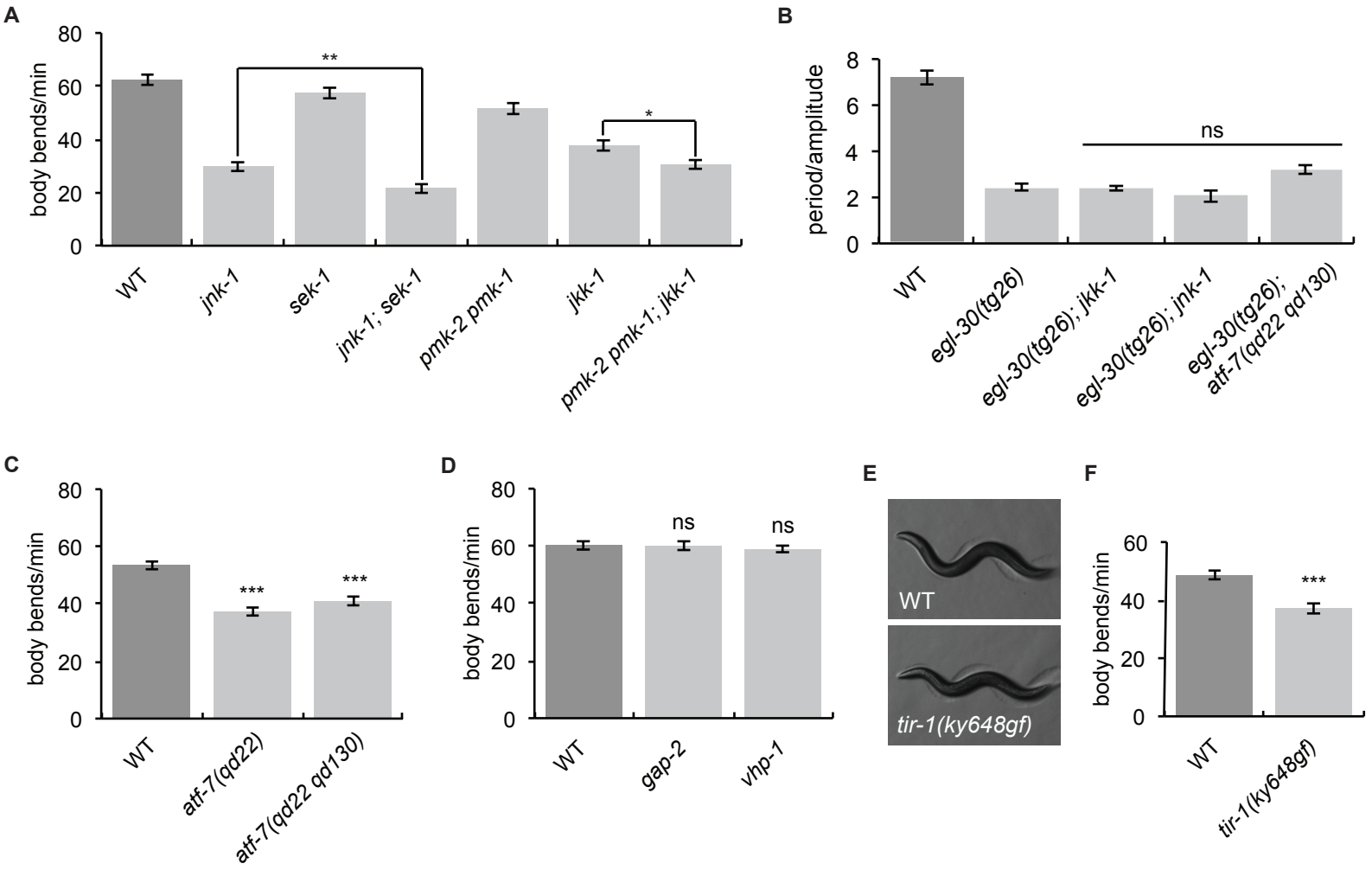

Figure S3. Locomotion of p38 and JNK MAPK pathway mutants

(A) *jkk-1* and *jnk-1* act in parallel to *sek-1* and *pmk-2 pmk-1*. The *jnk-1(gk7) sek-1(km4)* double mutant and *pmk-2(qd279 qd171) pmk-1(km25) jkk-1(km2)* triple mutants move more slowly than the respective individual mutants. **, p< 0.01, *, p<0.05. Error bars = SEM, n=20.

(B) Mutations in *jkk-1, jnk-1,* and *atf-7* do not suppress the loopy waveform of the activated Gq mutant *egl-30(tg26).* ns, p>0.05, error bars = SEM, n=5.

(C) Worms with gain-of-function or loss-of-function alleles of *atf-7* are slower than wild-type worms. ***, p< 0.001, error bars = SEM, n=20.

(D) Worms lacking *gap-2* and *vhp-1* move like wild-type worms. Neither *gap-2(tm478)* nor *vhp-1(sa366)* confers a slow locomotion phenotype. ns, p>0.05 compared to WT. Error bars = SEM, n=20.

(E-F) *tir-1(ky648gf)* animals do not have loopy or hyperactive locomotion. *tir-1(ky648gf)* worms have wild-type posture and are slower than wild-type animals. ***, p< 0.001, error bars = SEM, n=20.

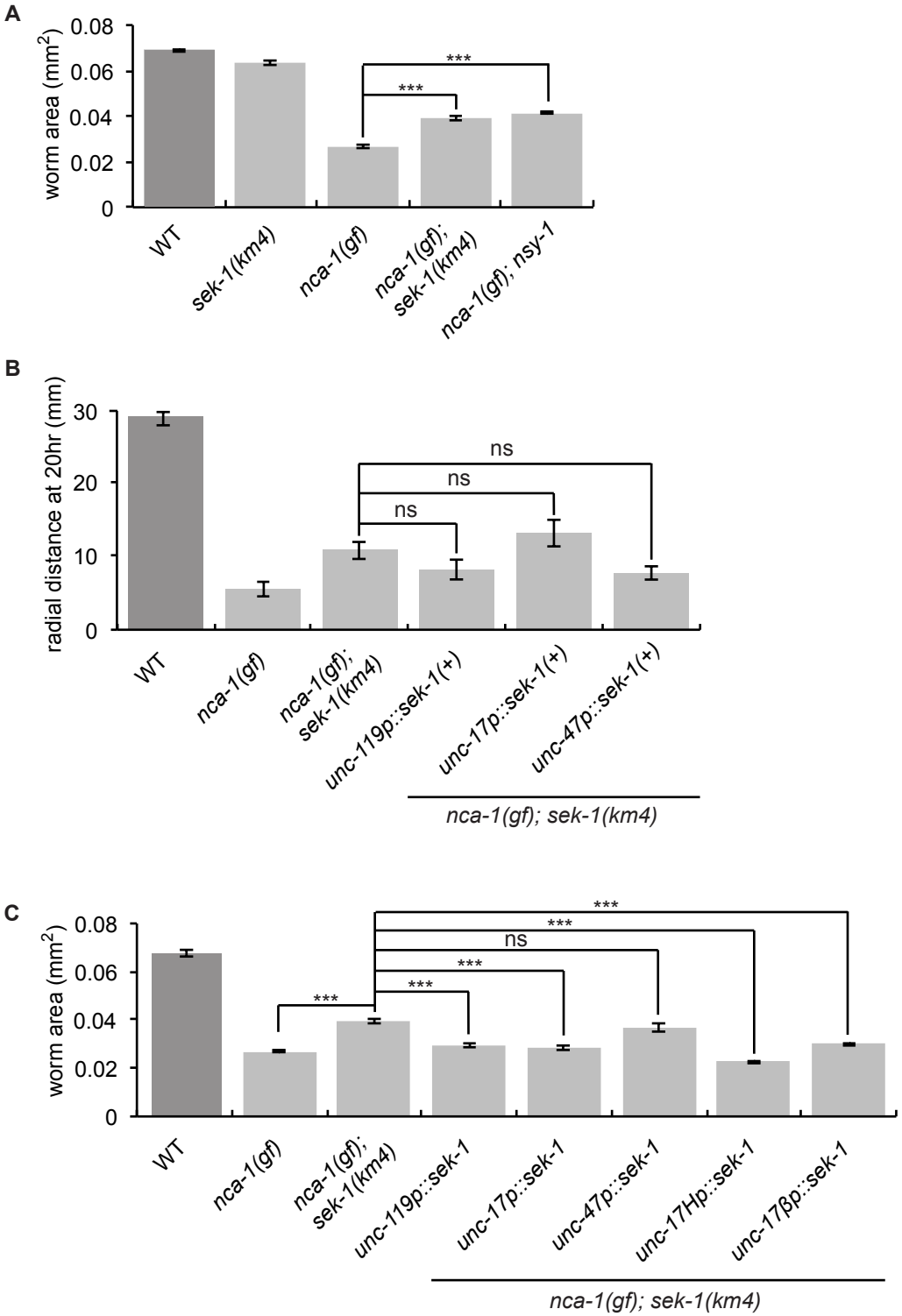

Figure S4. *sek-1* and *nsy-1* weakly suppress *nca-1(gf)*

(A) Mutations in *sek-1* and *nsy-1* suppress the small body size of *nca-1(ox352)* mutant worms. ***, p<0.001, error bars = SEM, n=10.

(B) None of the neuronal *sek-1* rescuing constructs reverse the radial locomotion phenotype of *nca-1(gf) sek-1(km4)* animals. ns, p>0.05. Error bars = SEM, n=19-24.

(C) *sek-1* acts in both head acetylcholine neurons and acetylcholine motorneurons to control the body size of *nca-1(gf)*. *nca-1(ox352) sek-1(km4)* worms expressing *sek-1* in all neurons (*unc-119p::sek-1(+)*), acetylcholine neurons (*unc-17p::sek-1(+)*), head acetylcholine neurons (*unc-17Hp::sek-1(+)*), or acetylcholine motorneurons (*unc-17βp::sek-1(+)*) have a similar size to *nca-1(gf),* but *nca-1(ox352) sek-1(km4)* worms expressing sek-1 in GABA neurons (*unc-47p::sek-1(+)*) are similar to *nca-1(gf) sek-1.*

***, p< 0.001; ns, p>0.05. Error bars = SEM, n=7-10.